ACTIVITY DEPENDENT PROCESSES GUIDE REMODELING AFTER TRAUMATIC SPINAL CORD INJURY

Carmen Katharina Denecke Muhr

Graduate School of Systemic Neurosciences

LMU Munich

Dissertation at the

Graduate School of Systemic Neurosciences

Ludwig-Maximilians-Universität München

February 2021

Supervisor
PD Dr. Florence Bareyre
Institute of Clinical Neuroimmunology
University Hospital and Biomedical Center
Ludwig Maximilian University of Munich

First Reviewer: PD Dr. Florence Bareyre
Second Reviewer: Prof. Dr. Martin Kerschensteiner
External Reviewer: Prof. Dr. Ronaldo Ichiyama

Date of Submission: October 20th, 2020
Date of Defense: February 3rd, 2021

TABLE OF CONTENTS

TABLE OF FIGURES

TABLE OF TABLES

ABSTRACT

Spinal cord injury causes a complete life change for patients and their social environment with severe economic, societal, and health implications. So far, there is no cure and only very limited treatment for patients suffering from spinal cord injury. Although central axons fail to regrow successfully after injury, incomplete spinal cord injury is accompanied by spontaneous but limited functional recovery. This recovery is attributed to compensatory neuroanatomical plasticity, where fibers remodel distal to the injury to establish new connections, so called neuronal detour circuits. Whilst various detour circuits in rodents are anatomically characterized in detail, the mechanisms of remodeling are not completely understood.

Activity dependent processes, such as N-methyl-D-aspartate receptor (NMDAR) signaling, cyclic AMP response element-binding (CREB) transcription, and neuronal activity itself, play a crucial role in the formation of neural circuits during embryogenesis. We analyzed the role of these processes in the cervical spinal cord, where the corticospinal tract has been demonstrated to sprout and contact novel target neurons after traumatic spinal cord injury. More specifically, we perturbed NMDAR signaling, (ii) suppressed CREB transcription, and (iii) silenced neurons with designer receptor exclusively activated by designer drugs (DREADDs).

Inhibiting NMDAR and CREB function in the cervical area during detour circuit formation both resulted in anatomically aberrant remodeling of the corticospinal tract. However, cervical circuitry remained unaltered when activity dependent processes were manipulated before spinal cord injury and after a mature detour circuit had already been established. These experiments demonstrate that spinal cord injury transiently opens a critical window of activity dependent plasticity, enabling detour circuit formation.

Furthermore, I argue that target selection during detour circuit formation after spinal cord injury is based on the neuron's relative level of activity. Firstly, this interpretation is based on our observation that global cervical silencing had no measurable effects whilst selective silencing of specific neuronal populations created an anatomically and functionally defective detour circuit. Secondly, within this defective detour circuit, the degree of neuronal silencing negatively correlated with the likelihood of that neuron to be contacted by corticospinal tract collaterals. With the help of a detailed literature analysis, I demonstrate similarities in plasticity between the developing CNS, the adult intact, and injured CNS and propose future experiments. Taken together, this thesis illustrates that activity dependent processes guide spontaneous detour circuit formation after spinal cord injury.

LIST OF ABBREVIATIONS

AAV – adenoassociated virus

BDA – biotinylated dextran amine

C1-7 – cervical level 1-7

CNO – clozapine-N-oxide

CNS – central nervous system

CREB – cyclic AMP response element-binding protein

CST – corticospinal tract

DIO – double-floxed inverse orientation

DREADD – designer receptor exclusively activated by designer drugs

eGFP – enhanced green fluorescent protein

NMDAR – N-methyl-D-aspartate receptor

PBS – phosphate buffered saline

PC – principal component

PCA – principal component analysis

PSN – propriospinal neuron

SCI – spinal cord injury

T1-13 – thoracic level 1-13

INTRODUCTION

Steroids, in particular, methylprednisolone, were considered the only viable treatment for spinal cord injury (SCI) for 30 years. [1] More recent investigations into the original clinical data, [2,3] however, deem the use of the drug for SCI treatment ineffective. [4] Some have even reported severe risks of methylprednisolone treatment, such as the development of pneumonia or sepsis. [2,3]

Steroids against SCI present an example where preliminary results on functional improvements without anatomic data impacted treatment approaches too soon; they demonstrate the necessity of fully understanding natural pathological processes before inferring intervention effectiveness. If possible, the failure or limitations of interventions should be demonstrated before reaching expensive and lengthy clinical trials. In research on SCI, it is, thus, crucial to discern natural pathological processes and the central nervous system's (CNS') attempt to recover from these to optimize treatment effectiveness. In this dissertation, I will argue that SCI is a devastating disease with far reaching implications for those affected and society as a whole. I will present current knowledge on pathological processes induced by SCI and the CNS' natural ability to remodel rather than regenerate following injury. Our experiments elucidate the role of neuronal activity in the process of remodeling. Finally, I will critically discuss these results and suggest future directions for SCI research on remodeling.

EPIDEMIOLOLGY AND SYMPTOMS – SCI IS A DEVASTATING DISEASE

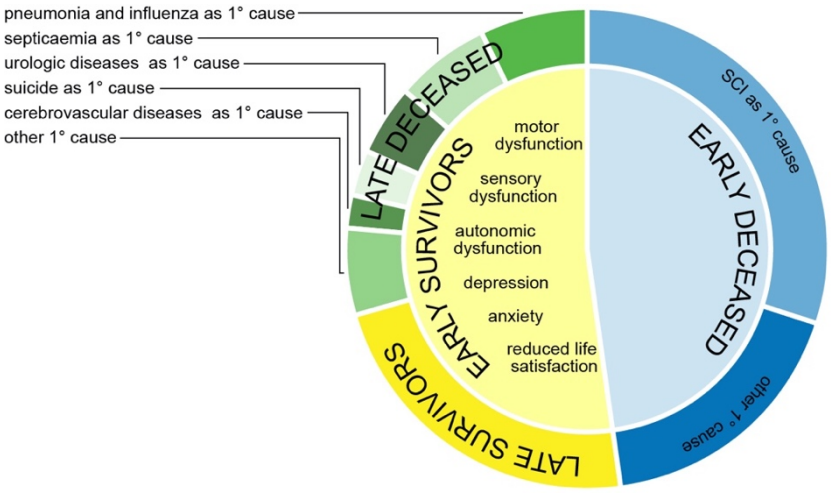

FIGURE 1 Short-term and long-term case fatality rates for SCI. Almost half of the afflicted patients die before the end of initial hospitalization (early deceased). The majority of these cases list SCI as the primary cause of death in the autopsy protocol. [6] When patients do survive, they develop severe physical and psychological symptoms, eventually leading to high long-term case fatality rates (late deceased). Death caused by pneumonia and influenza, septicaemia, diseases of the urinary tract, suicide, and cerebrovascular diseases are significantly increased in this SCI population when compared with a non-injured population of the same age. Long-term case fatality rates were calculated from standardized mortality ratios taken from ref. [7], which analyzed deaths in the SCI afflicted later than 18months after injury. Late survivors are SCI patients with the same life expectancy as individuals in a non-injured population. All data are based on studies conducted in developed countries. Case fatality rates might be higher in less developed areas.

With 40-80 in a million new cases of SCI each year, [5] SCI is a universal disease, crossing borders of nationalities, age groups, and economic status when afflicting new patients. Case fatality of SCI before the end of initial hospitalization has been reported as 48%, with the majority of patients dying upon injury (Figure 1). [6] According to autopsy protocols, SCI is considered the primary cause of death in more than half of these fatal cases. [6] Although already alarming, even higher SCI fatality rates of more than 50% are reached when including deaths caused by

later secondary pathological effects or cases of suicide, one of the leading causes of death after surviving the initial injury (see “late deceased”, Figure 1). [7]

Surviving the initial critical phase comes at the staggering personal cost of countless psychological symptoms and physical impairments. SCI severely affects informational exchange between the spinal cord and brain. The lost information can be of motor or sensory nature, leading to physical impairments below the injury site for the patients’ entire lives, with little prospect of relief. These impairments can be accompanied by a loss of autonomic functions, creating, for example, bladder, bowel, and sexual dysfunction. Patients, hence, remain dependent on social support, impacting not only their own quality of life but also that of their friends and family. Psychological symptoms can develop, ranging from mild changes, such as increased levels of distress and decreased levels of reported life satisfaction, [8] to additional severe conditions, like anxiety or depression. [9]

With largest traumatic SCI incidence rates in individuals in their twenties, [10] they pose a large economic burden on society. A recent estimation of the lifetime economic burden of one SCI individual in Canada amounted to $1.5-3 million, depending on the severity of impairments caused by the injury. [11] These costs include direct costs, i.e., medical expenses to relieve symptoms of SCI, and indirect costs, caused by a loss of the patient’s productivity and income. Epidemiological analyses of SCI illustrate the necessity for and lack of appropriate SCI treatment, which could reduce the large psychological, physical, and socioeconomic burden, impacting patients themselves, their families, communities, and society.

CLASSIFICATION OF TRAUMATIC SCI – INJURY LOCATION DETERMINES IMPAIRMENTS IN HUMANS AND RODENTS

SCIs vary across patients and prompt different phenotypes. Neurologic deficits induced depend on injury location and severity, i.e., which vertebra covers the injury and which anatomical components of the spinal cord is damaged.

The spinal cord, in humans, extends from the cervical vertebra 1 to the lumbar vertebrae 1/2 [12]; the more rostral the injury, the more detrimental the clinical outcome. Most cases of SCI occur in the cervical spinal cord due to its high mobility with small vertebrae and, hence, larger direct target areas for impact sources. [13] Unfortunately, injuries of this type also induce the strongest physical impairment (Figure 2A); often tetraplegia/quadriplegia develops – paresis of all four limbs. Injuries of lower spinal cord levels can induce paraplegia – paresis of the lower body.

The completeness of the injury also impacts the severity of physical symptoms that manifest after SCI. Fortunately, in comparison to incomplete SCIs, complete lesions have become less prevalent since the mid 20th century. [14] This reduction is likely explainable by a superior emergency response, where

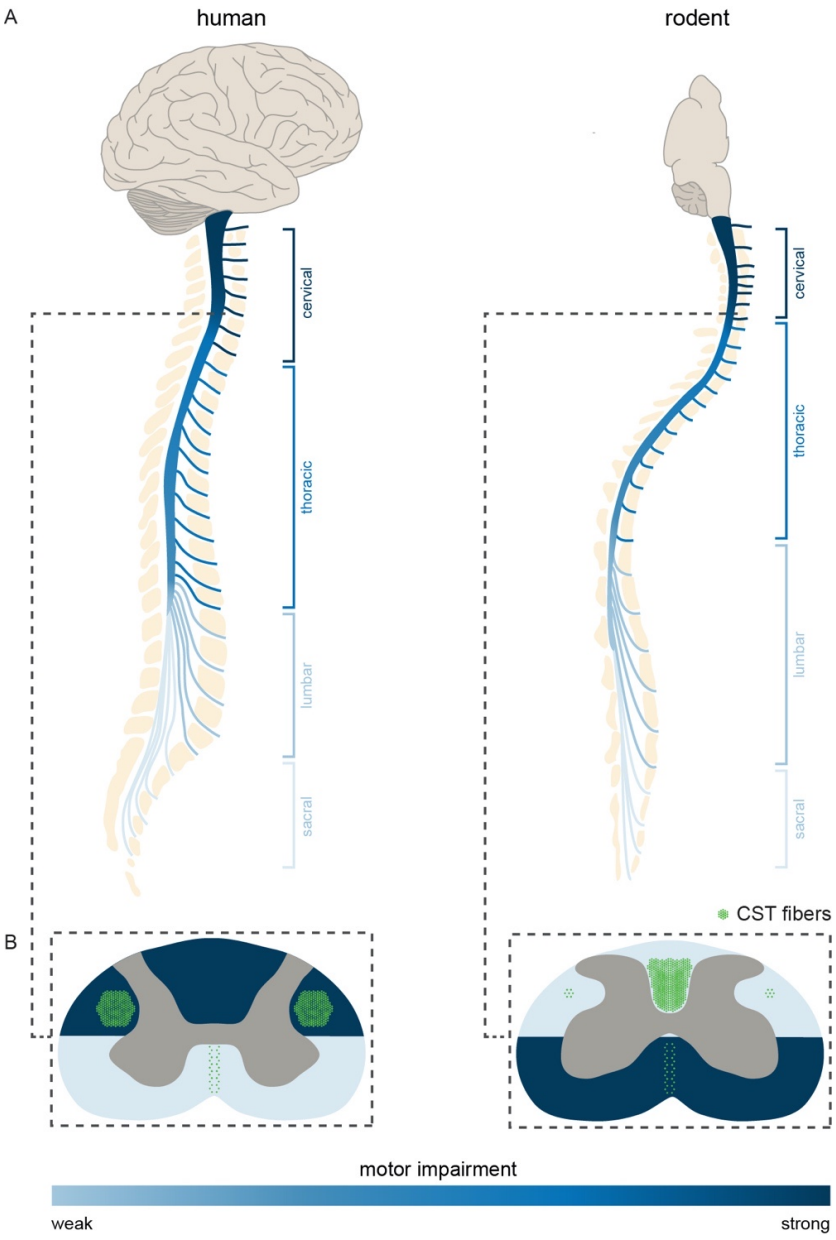

FIGURE 2 Anatomy of the human and mouse spinal cord, illustrating the relationship of injury location and symptom severity. The whole spinal cord **(A)** and its zoomed in coronal sections **(B)** are color coded in shades of blue where the darkest shade indicates that a lesion to this area would lead to the severest motor symptoms and the lightest shade to the mildest symptoms. The mouse vertebral column is based on a micro CT scan, with permission from ref. [185]. The human vertebral column is adapted, with permission from ref. [186].

secondary injury is avoided by immobilization of the affected individuals, and improved diagnosis based on the integration of anatomic with behavioral data.

The relationship between injury completeness and motor outcome is not linear. Surgically induced spinal cord transections for intractable pain relief have provided insight into the motor impairments caused by different types of injuries. [15,16] For example, a complete transection of the human ventral spinal cord at the thoracic level induces no or very minimal impairments in motility, whereas a mere unilateral transection of the posterolateral column, a relatively small strand of the dorsal spinal cord, leads to a complete paralysis of the affected limb. [16] Thus, the localization of the injury within a spinal cord transection determines which neural tracts are transected and, hence, which symptoms manifest.

LESIONING THE CST

In humans, transections of the posterolateral column induce such severe impairments because it includes the majority of the corticospinal tract (CST), the lateral CST. [12] Due to the importance of the CST for human motor control, our experiments in rodents focus on exactly this descending motor tract. Aside from the lateral CST, a smaller medial CST runs in the central column of the spinal cord (Figure 2B). [12] Both components originate in several areas of the cortex. [17] The motor cortex is somatotopically organized, so that it consists of forelimb and hindlimb motor areas, responsible for the activation of

different sets of muscles. Restoration of CST function after injury would lead to grave improvements in symptoms of patients.

In rodents, the CST consists of three components, a dorsomedial, a ventromedial, and a dorsolateral component (Figure 2B). [12] The vast majority (~95%) of all CST fibers run in the dorsomedial component, in the ventral part of the dorsal column, rendering all CST fibers after an injury to this area almost completely transected. Contrary to observations in humans, rats with a lesioned dorsomedial CST do not exhibit a complete paralysis of limbs but merely difficulties in fine movements, such as paw placement. [18] When assessing the effect of interventions to increase CST functionality after injury, fine motor skills have to be considered in rodents and gross motor skills in human patients.

PATHOPHYSIOLOGY – SCI INDUCES A CELLULARLY DAMAGING CASCADE

SCI follows a biphasic pathophysiological process, composed of a primary and a secondary injury. The primary injury is the initiator - the mechanical injury that is caused by an insult on the back, its resulting broken bone or intervertebral disk displacement, and the contusion, compression, distension, or, in rare cases, transection of the spinal cord. Ascending and descending pathways, neuronal cell bodies, glial cells, blood vessels, and the dura can be harmed in the process.

The primary injury, then, cascades into a long-lasting, progressive secondary injury, which is characterized by cellularly damaging or even lethal processes (Figure 3A). While the primary injury can merely be prevented, if at all, the secondary injury can be modified by disease interventions. In the following, I will outline some of the major challenges the spinal cord faces during secondary injury and use examples of pathophysiological modulation in rodents to illustrate the complexity of the CNS' response to SCI.

As previously indicated, tract damage composed of axons determine the functional outcome following SCI. Understanding the processes in which axons dieback after injury is, hence, crucial for designing SCI treatment. After injury, axons remain stable for a short period. [19] *In vivo* imaging of the real-time effects of axonal transection has revealed that two minutes after injury, though, axons already start dying back through different processes: (1) pore-induced axonal loss, (2) axonal retraction, and (3) Wallerian degeneration. During pore-induced axon loss after contusion, mechanopores in the membrane allow the sudden influx of calcium, causing swelling, and eventually fragmentation of the entire axon. [19] Pore-induced axon loss and axonal retraction both happen only up to hours after SCI and damage the entire axon. [20,21] In contrast, Wallerian degeneration occurs up to weeks later and only affects part of the axon that is distal to the injury, without connection to the cell body. [20,22] Wallerian degeneration has also been seen to spread to intact, uninjured axons neighboring the SCI. [23] The primary injury alone, hence, is not conclusive of the lost connections between brain and spinal cord. The true extent of denervation in rodents will only manifest weeks after the insult to the spinal cord.

Although some axons may remain intact following SCI, they fail to conduct signals efficiently. Oligodendrocytes, which usually isolate axons with myelin and streamline signal conduction, also

undergo apoptosis following SCI. [24,25] This cell death causes demyelination up to weeks after the primary injury. One study has shown that demyelination exposes axons to further damage and could induce axonal degeneration later on. [26]

As aforementioned, primary injury can not only damage nervous tissue but also blood vessels that usually supply the injured region of the spinal cord with nutrients and oxygen. Vascular damage results in reduced blood perfusion of the affected region, so called ischemia. Ischemia leads to a quick depletion of the CNS' limited energy reserves and the loss of ionic homeostasis, eventually causing increased cell death in the injured spinal cord.

Damage to blood vessels also harms the blood-brain barrier, [27–29] allowing immune cells to enter the injury site and subsequently aiding in a severe, persistent inflammatory response. Manipulating the immune response in the spinal cord after injury has generated seemingly conflicting observations, where either positive or negative effects on disease outcome were reported. [30,31] For example, microglia are one of the first immune cells to respond to SCI, and their activation has long been considered detrimental to disease pathology. Several studies could show that antagonizing cytokines produced by microglia activation reduces tissue damage and apoptosis following SCI. [32–34] New research, however, indicates that microglia can be activated disparately, resulting in a neuroprotective impact on disease outcome. [35,36] Hence, the immune cell's effect on SCI depends on the pathway by which it is activated and cannot be bluntly declared as good or bad for the disease.

Research on the immune response following SCI has also revealed the determinant role of genetics and age in disease pathology. Different rodent strains vary in their magnitude or chronology of immune response. For example, C57Bl/6 mice, a mouse strain used in this thesis' experiments, activates an increased number of microglia following SCI when compared to another common mouse strain, BALB/c. [37] Immune responses to SCI are also influenced by differences in age. [38,39] Pathological differences due to a genetic or age-related heterogeneity need to be considered in the development of treatment and their appropriate use by spinal injured individuals.

Cell death triggered by ischemia and the primary injury causes the excessive release of glutamate, initiating excitotoxicity. [40] When applying glutamate in a trauma comparable dose on healthy spinal cords, one can reproduce secondary injury-like neuronal cell death. [41] This lethality is explained by glutamate's hyperstimulation of neurons and glia cells as well as the resulting excessive uptake of calcium into the affected cell. High levels of intracellular calcium harm the cell or the axon during the aforementioned pore-induced axonal loss by activating enzymes that destroy crucial cell structures or eventually cause apoptosis. [42,43] Calcium induced glial and neuronal death increases extracellular glutamate levels even further, initiating a vicious cycle of excitotoxicity. Scientists have shown that breaking the cycle of excitotoxity by blocking glutamate receptors, and more specifically, N-methyl-D-aspartate receptors (NMDARs) with the antagonist MK801, right after SCI, leads to a positive behavioral outcome in rats. [44] As explained later in the results section of this dissertation, we have observed

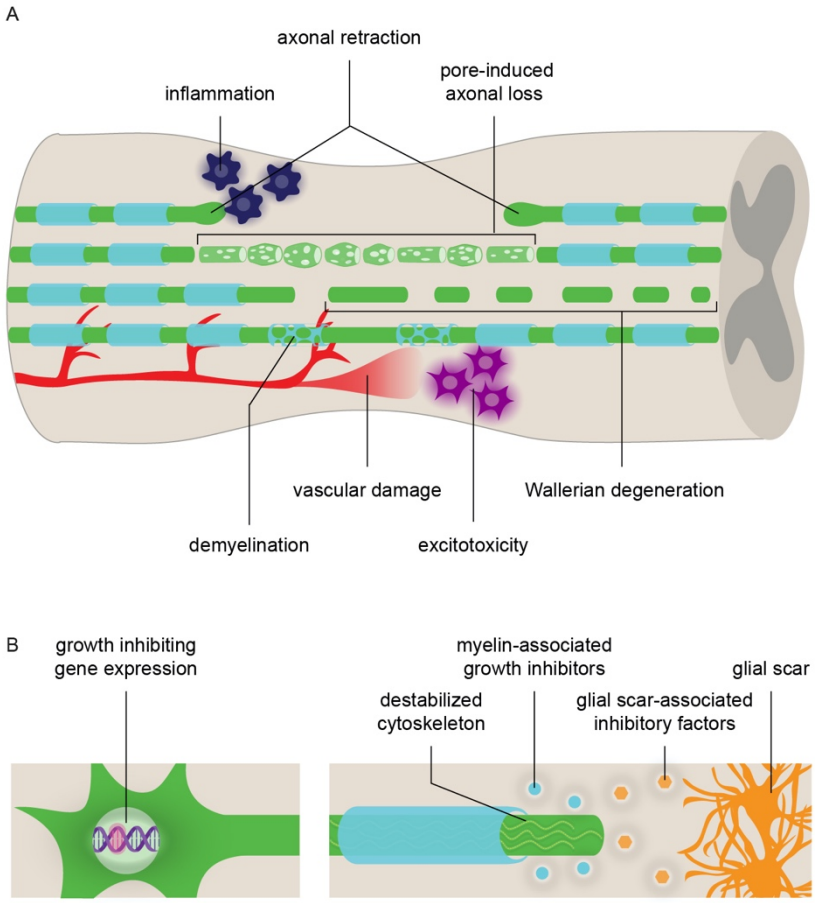

FIGURE 3 SCI induces a cellularly damaging secondary injury, which impedes on regenerative attempts by the CNS. **(A)** Processes supporting cellular damage after SCI. **(B)** Challenges for axonal regeneration after SCI.

contrary effects of MK801, where the drug worsened SCI pathology. These conflicting results illustrate the importance of intervention timing. In our study, we administered the drug when excitotoxicity had already worn off.

To conclude, knowledge on secondary injury pathology highlights the severity and complexity of this damaging cascade and has taught valuable lessons for future research: (1) researchers should defer from the simplification of evaluating certain pathophysiological phenomena as either good or bad, (2) genetics and age impact SCI pathology, and (3) timing as well as localization of putative interventions are crucial.

DAMAGED AXONS FAIL TO REGENERATE SPONTANEOUSLY & INTERVENTIONS ARE CHALLENGING

Aside from reducing the damaging effects of the secondary injury on SCI outcome, rebuilding lost connections via axon regeneration could also induce recovery. In contrast to lesions to the peripheral nervous system, the CNS fails to reinstate original circuitry after injury and degeneration, impeding functional recovery. *In vivo* imaging in mice has provided great insight on the central axons' severely limited regenerative processes in response to injury. A minority of proximal axons, i.e. the part of the axon still attached to the cell body, grows hours to days following the lesion. [20,45] This outgrowth, however, is merely an unsuccessful attempt to reinnervate previously lost connections. The majority of axonal sprouts grow aimlessly and have a severely reduced caliber with many side branches. [20,23] In addition, oligodendrocytes try to remyelinate axons after SCI but only generate abnormal, thin sheaths. [24] More mature seeming axons with straighter trajectories might reach the initial lesion site a week post injury only to find their distal end completely degenerated with no opportunity to reconnect. [45]

Both the central axon's intrinsic and extrinsic composition hinder central axon regeneration after SCI, which can be elucidated by two experiments. First, when solely changing the environment of lesioned central axons by implanted regeneration-supportive peripheral nerve grafts, a substantial amount (20%) of central axons can regenerate successfully along the graft. [46] A second set of experiments demonstrates that intrinsic regeneration processes can be activated independently from the spinal cord's environment. Dorsal root ganglion neurons with a central branch projecting to the spinal cord can be conditioned to regenerate if their peripheral branch was lesioned beforehand. [47] In the following, I will first briefly summarize SCI interventions in rodents tackling obstacles of regeneration (Figure 3B), rooted in a regeneration-hostile environment and the intrinsic inability to regenerate. Secondly, I will discuss potential shortcomings of those interventions.

MODIFYING THE EXTRINSIC REGENERATION INHIBITORY MILIEU

While peripheral axons, whose conduction is isolated by Schwann cells, can regenerate, central axons, wrapped in myelin sheaths, fail to regenerate. Likewise, cultured neurons do not grow axons on top of myelin extracts but exhibit high affinity for axon outgrowth on nerve explants containing Schwann cells. [48] The first molecule found to be responsible for myelin's inhibitory impact on axonal outgrowth was Nogo-A, which was soon followed by others, such as myelin associated glycoprotein and oligodendrocyte myelin glycoprotein. Approaches neutralizing myelin-derived growth-inhibitors have been deemed successful by inducing axon regeneration beyond the spinal cord lesion in multiple settings. [49–52]

Peripheral regeneration does not only profit from the absence of myelin but also from the presence of Schwann cells and their secretion of growth-promoting neurotrophic factors. Thus, transplanting Schwann cell grafts into the spinal cord can remyelinate severed axons and induce limited regeneration of thicker and more robust central axons. [53] The Schwann cells' secretion of growth-promoting neurotrophic factors usually guides and promotes axon outgrowth during development and after peripheral injury. [54–56] When added to injured spinal cords, a myriad of neurotrophic factors can recapitulate developmental growth processes. [57–61] Instead of mere topical administration of growth factors, implanted Schwann cells can also be genetically engineered to hyper-secret further growth factors yielding strongest axon regeneration after SCI. [62,63]

Glial cells are also an important component of the change in extracellular milieu after SCI; they form a scar around the primary injury to seal it and isolate damage. [64,65] However, the glial scar also creates an impenetrable barrier for axonal regeneration due to its density and release of inhibitory factors. [66–68] A well-studied inhibitory family is chondroitin sulphate proteoglycans, which has been neutralized with the enzyme chondroitinase ABC [69] or by genetically removing enzymes crucial for the factors' proper mechanism of action. [70,71] Neutralizing the glial scar associated inhibitory factors can aid in axon regeneration of the injured proximal axon stumps.

MODIFYING THE INTRINSIC CAPABILITY TO REGENERATE

Neural stem cells can be a supportive structure for the regeneration of host axons. Likewise, neural stem cells have been used to replace previous connections. For example, when transplanting neural stem cells into the spinal lesion within a supportive fibrin matrix, neural stem cells can grow axons with lengths up to 25mm, which outshines all previous interventions yielding outgrowth of 1-2mm. [72] A neural stem cell approach can, hence, aid in modifying the regeneration inhibitory intra- and extracellular.

The contrast in regeneration capabilities of peripheral and central axon is based on different gene expression after injury. Gene expression analyses have provided great insight into how certain signaling pathways can activate an axonal regeneration-enabling program after peripheral nerve injury. Applying knowledge from the peripheral nervous system to the injured CNS by targeting genes involved in growth associated signaling pathways has proven promising. For example, manipulating growth supportive transcription factors, which coordinate the expression of multiple genes, in central neurons of the injured spinal cord has promoted axon outgrowth in a myriad of settings. [73–77] Studies where growth associated transcription factors are upregulated could also illustrate that regeneration is a dynamic process. Upregulating the transcription factor STAT3 in injured central axons, for example, only aids in the initiation but not the maintenance of regeneration. [73] This interpretation was further supported by deleting STAT3 in regenerating peripheral nerves where axonal outgrowth was delayed but not completely abolished. [73] The study indicates that gene expression highly varies during phases of regeneration; it stresses the importance of time conscious analyses and poses another challenge for successful intervention to increase regeneration.

An additional distinction between injured central and peripheral axons is the cytoskeleton's stability. The cytoskeleton, responsible for the transport of subcellular machinery, e.g. organelles, new cytoskeletal components, lipids, and proteins, allows for the typical growth cone formation and thereby axon outgrowth following peripheral nerve injury. However, microtubules, a major component of the cytoskeleton, destabilize in central axons upon injury. [78] Administering drugs that stabilize microtubules has been shown to prevent axonal degeneration and support regeneration after SCI. [79–81]

ISSUES WITH REGENERATION SUPPORTIVE INTERVENTIONS

Although all previously outlined interventions could boldly be summarized as yielding increased regeneration following SCI, the extent of those effects is quite limited. Neutralizing the growth-inhibitor, Nogo-A, for example, only increases regeneration in 5% of the injured axons [49] – a minimal proportion compared to an astounding 90% of naturally regenerating peripheral axons. [82] Furthermore, outgrowth length in the few axons that do regenerate is also only increased minimally through intervention. In humans, regenerating spinal cord axons need to overcome even larger distances to induce functional improvement, which poses an additional challenge for the effectiveness of already limited regeneration-supportive interventions.

Axonal outgrowth by itself cannot lead to functional improvements and is, therefore, not the sole determinant of functional recovery. The leap in regeneration after neural stem cell transplantation [72] or

after the combination of several interventions [83] did not cause a leap in behavioral benefits when compared to results from previous interventions. In fact, many experiments with minimally increased axonal outgrowth could, nonetheless, link it to some positive behavioral effect after SCI, such as improved motor recovery. A possible explanation for this phenomenon is that regeneration length does not correlate highly with motor recovery, and only a small proportion of a motor tract needs to be intact for it to function properly. These observations demonstrate that the search for successful intervention needs to move beyond sheer axonal outgrowth and deal with the establishment of original neural circuitry to achieve complete functional recovery. Thus, besides stimulating regeneration, neurons need to survive and regenerate with direction, where contacts onto newly denervated neurons are restored. All these components are required but by themselves not sufficient for successful intervention.

When evaluating the success of interventions, functional data are indispensable. Functional data can be acquired by measuring neuronal activity, such as electrophysiology, histochemistry or *in vivo* calcium imaging, or can be represented directly with behavioral experiments. Still, increased behavioral recovery itself does not prove that they were caused by the investigated anatomic alterations. Instead, re-lesioning or silencing experiments are necessary to demonstrate a causal relationship between a specific anatomic alteration and behavioral outcome.

An alternative cause for functional recovery induced by regeneration supportive interventions could be the alteration of disregarded neural circuits as an off-target effect. In addition to the regeneration of central injured axons after SCI, spared axons might reorganize. In fact, many studies could show how increasing regeneration with established growth-enhancing interventions was concomitant with increasing remodeling. Reportedly, enhancing the growth associated mTOR pathway, [76] upregulating transcription factor KLF7 [74] or STAT3, [73,84] neutralizing a glial scar associated inhibitory factor with chondroitinase ABC, [85] and neutralizing myelin associated growth inhibitor NogoA [50] have all been shown to also boost remodeling. These modulations indicate that axonal outgrowth processes in regeneration and remodeling might underly similar mechanisms. Some studies even failed to induce any increased regeneration in injured axons after SCI by neutralizing all three myelin associated growth inhibitors [86,87] and could only demonstrate increased growth of spared axon collaterals distal to the injury. [87] In order to completely understand an intervention's effect on SCI pathology, it is crucial to examine alterations in regeneration, remodeling, and behavior. Former re-lesioning studies or state-of-the-art silencing experiments, as used in this thesis, present a powerful tool in investigating which anatomic alteration is responsible for behavioral recovery.

To summarize, axons in the spinal cord fail to regenerate after injury due to extrinsic factors and intrinsic incapability. Much focus has been directed towards interventions that aid in overcoming these barriers and achieving regeneration. However, regeneration is only one aspect of anatomic alteration that could aid in behavioral improvements. Tackling remodeling of intact neural circuits distal to the lesion alongside its destabilized cytoskeleton, inhibitory glial scar, and damaging cytokines is a promising approach for designing successful SCI intervention.

THE HUMAN CNS REMODELS CHRONICALLY AFTER SCI

Patients suffering from incomplete SCI exhibit limited spontaneous recovery without intervention. This limited recovery can be strengthened by physiotherapy. Patients with treadmill training, for example, regain rhythmic patterns of locomotor muscle activation and decrease their muscle spasticity. [88] In total, treadmill training by itself increases the number of independent walkers by 42% in patients with incomplete SCI. [89] These observations are certainly not based on, as in the previous chapter described, failed regeneration nor can they be explained entirely by increased muscle strength, but instead result from different types of CNS remodeling. Although SCI severely restricts the transmission of signals between the brain and spinal cord, a bulk part of neurons involved in the healthy transmission process survive and continue to respond to synaptic input. Intact neurons present a powerful possibility in overcoming signaling barriers and inducing recovery of function after SCI by CNS remodeling.

For the purpose of this thesis, I define CNS remodeling as a chronic response to SCI where uninjured neuronal circuits are altered, resulting in a long-term increase in activation of certain central neurons or entire areas. These uninjured circuits can be altered structurally and/or functionally. Structural remodeling entails changes in diameter or length, viz. sprouting, of axon collaterals or dendritic branches, where new synapses and, hence, new circuits can be formed. Functional remodeling can be achieved by changes in neuronal excitability, synaptic strength or changes in glial activity.

In humans, studies could verify the occurrence of remodeling after SCI but not determine how it developed. Specifically, changes in activation of certain CNS areas in SCI patients in comparison to a healthy population can be measured with non-invasive techniques such as positron emission tomography, [90] functional magnetic resonance imaging, [91–97] or transcranial magnetic stimulation. [98–101] Invasive techniques used in rodent studies are clearly not applicable to human patients, which averts inferences on the structural or functional nature of remodeling.

Many neurons in the brain are not directly affected by SCI, and yet some can reorganize upon injury. These remodeling effects have been shown to increase with exercise. For example, motor recovery in patients with incomplete SCI following treadmill training correlates with an increase in CST connectivity. [102] Several other studies have compared healthy and SCI subjects to show increased activation of motor areas during actual or even imagined movement. [90,94–96] This increase in activity also includes completely novel activation of brain areas that are inactive during movement in healthy subjects. For example, motor cortex areas that activate during movement of functional body parts, rostral to the SCI, have been observed to expand into a deafferented part of the motor cortex formerly activated for the movement of now paralyzed body parts. [93] Similarly, studies using transcranial magnetic stimulation show that an expanded area of the motor cortex can excite motor neurons in muscles of functional body parts. [99–101] It is hypothesized that the activation shift in the cortex could aid in maximizing outputs of movement since it has been shown to increase with rehabilitation. [97,98] These experiments demonstrate the functional benefit this type of remodeling can offer.

However, remodeling upon SCI does not necessarily translate into recovery but can have negative consequences, like observations in remodeling of the somatosensory cortex revealed. Similar

to the motor cortex, the somatosensory area's lost input from denervated body parts are replaced by input from neighboring sensorially intact body regions. [91,92] One study found that the extent of this somatosensory remodeling correlates with neuropathic pain of the denervated body parts. [91] The generation of deafferentation pain following SCI shares similar mechanisms with phantom limb pain after amputation. [103,104] These human experiments investigating remodeling in the somatosensory and motor cortex following SCI illustrate how remodeling can be an obstacle or a great asset in trying to relief SCI related symptoms.

KNOWLEDGE OF CNS REMODELING IN RODENTS AIDS IN OPTIMIZING SCI INTERVENTIONS

The potential of the animals' CNS to undergo spontaneous remodeling without intervention following SCI has been long established and repeatedly reaffirmed. Early experiments also provided evidence for remodeling through functional data, i.e. rehabilitation after SCI. Researchers could help cats regain stepping abilities after complete transections by training them on treadmills. [105,106] Soon, studies showing the positive effect of locomotor training on SCI recovery in rodents followed. [107–109]

In contrast to human studies, rodent studies can clearly include more invasive techniques, which help in widening our understanding of remodeling. Rather than making inferences on remodeling upon changes of activation in the CNS, researchers can visualize entire detour circuits formed through remodeling processes directly. Below, methodological differences within rodent studies investigating SCI induced remodeling are outlined concerning the injury model, behavioral assessment, and tracing method.

METHODOLOGY OF RODENT REMODELING STUDIES

When studying remodeling, induced SCIs need to be incomplete. Some remodeling studies use a contusion injury model as it is most clinically relevant; it mimics most injuries in humans where a force from outside of the body compresses the spinal cord. Varying the strength, size, and duration of the compressive force defines the extent of SCI. Alternatively, most remodeling studies, like the ones presented in this thesis, have opted for an incomplete transection. Transecting the spinal cord allows researchers to controllably injure a specific part of the spinal cord where they are not limited to a dorsal approach, but could also, for instance, perform a lateral hemisection. Although this injury model does not mirror what occurs in most human patients, it presents a very powerful approach due to reproducibility.

The largest advantage of animal models in studying remodeling after SCI is our ability to visualize remodeled neuronal networks with fluorescence microscopy. Scientists have countless methodological options to choose from when deciding how to make remodeled networks fluorescent. Bareyre and colleagues, for example, have opted for creating a transgenic mouse line that expresses a fluorescent protein in the entire CST. [110] The oldest and simplest method to track any neuronal projections, though, is the application of molecular tracers. With a local injection into the region of interest, neurons take up

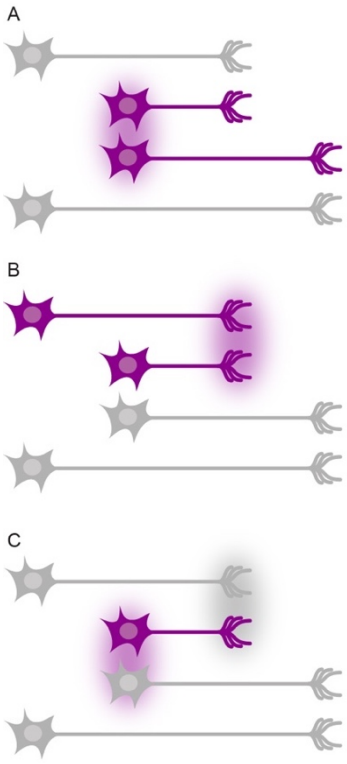

FIGURE 4 Tracing methodology applied in remodeling studies after SCI. **(A)** Anterograde tracer/virus illustrates where a labeled population sprouts. **(B)** Retrograde tracer/virus illustrates which populations sprout in a particular area. **(C)** Combining a cre-dependent anterograde virus with a retrograde cre-inducing virus allows for intersectional labeling; it specifically labels neurons with a soma at the anterograde viral injection and projections at the retrograde viral injection. Magenta halo: injection site of tracer with fluorophore, gray halo: injection site of cre-inducing retrograde virus.

the tracers and transport them antero- or retrogradely over a time course ranging from days to weeks. Whereas anterograde tracers are transported from the soma to axonal endings (Figure 4A), retrograde tracers move in the opposite direction (Figure 4B). Injecting anterograde tracers, such as biotinylated dextran amine (BDA) allows for the visualization of entire axonal projections and where they remodeled. In the case of the motor cortex, adjusting the injection coordinates along the mediolateral and rostroventral axis, even results in distinct labeling of either the hindlimb or forelimb CST. Retrograde tracers, such as hydroxystilbamidine (FluoroGold^{TM}), can show which neuronal populations after SCI sprout at the injection site. Applied together, one can prove whether the anterogradely labeled sprouting collaterals form contacts onto a retrogradely labeled neuronal population after SCI.

Aside from molecular tracers, researchers' tracer toolbox also includes recombinant viral tracers that drive the expression of fluorescent proteins, such as the most commonly used adenoassociated virus (AAV). Similar to molecular tracers, static viral tracers can label single connections anterogradely or retrogradely (Figure 4 A and B); they are, thus, a great tool to determine sprouting of one neuronal population. [111] Moving beyond tracing, viral vectors are a powerful tool to genetically manipulate neurons in remodeling circuits.

Moreover, viral tracers can target very defined neuronal subtypes by combining site-specific recombinase technology, such as the cre-lox recombination system. The effect of cre recombinase binding to its lox sites depends on the relative orientation of the lox sites. In this thesis, for example, we use a mouse line with two lox sites oriented in the same direction surrounding a gene of interest. When cre recombinase expression is induced by AAV injection, our gene of interest is excised. In addition, we make use of a double-floxed inverse orientation (DIO) AAV where an inverted fluorophore sequence is surrounded by opposing lox sequences. If cre expression is, then, induced with another AAV or a transgenic mouse line, the inverted fluorophore sequences will be flipped, and the fluorophore is successfully expressed. For intersectional labeling, we combined the anterograde DIO-AAV with a retrograde cre-AAV. Thereby, only neurons with a soma at the site of anterograde AAV injection and axon terminals at the site of retrograde AAV injection will be manipulated or traced (Figure 4C).

Evaluating functional rather than just structural remodeling in rodents can be, amongst others, accomplished by electrophysiological recordings or markers of neuronal activity, such as a staining for the synaptic marker synapsin. The most direct way of proving the functional relevance of underlying structural remodeling is behavioral assessment. Naturally, functional changes due to motor tract remodeling involve motor rather than sensory behavior. The oldest motoric assessment applied in motor

tract remodeling studies is the Basso, Breasie and Bresnahan locomotor scale for rats and the Basso Mouse Scale. Researchers classify motor recovery on a point scale that evaluates rather gross hindlimb function. [112,113] It is, hence, used in studies with thoracic injuries where only hindlimbs are affected and changes in motor skills are severe. The subjectivity introduced by the researcher's evaluation make the data more variable. [114] Another test for locomotor recovery is the horizontal ladder walking test. [114] In this test, mistakes a mouse makes when crossing a horizontal ladder are counted. It is an easy and cheap test, which is widely applied in SCI remodeling studies. The readout in these studies, however, is limited. New computer assisted gait analyses benefit from the high sensitivity in vast types of readout, from fine to gross motor changes, and the reduction of inter-rater variability. A three-dimensional analysis of locomotion is achieved via camera recordings of the rodent from multiple angles. [115] This method allows tracking of entire locomotor profiles after SCI. Yet, three-dimensional recordings plus analysis require expensive equipment and are time consuming. To assess the behavioral effect of our intervention on remodeling in this thesis, we have chosen another objective and sensitive, though cheaper, computer assisted gait analysis: the CatWalk. [116] In the CatWalk test, rodents walk on a specially illuminated glass platform that is recorded from below. This setup together with computer aided extraction allows the analysis of rodent paws placed on the ground.

The variety in parameters, from print area through stride length to speed, generated by computer assisted gait analyses like CatWalk, comes with a downside of a high-dimensional, large dataset. Reducing the dimensionality with a principal component analysis (PCA) aids in interpreting the data by summarizing the biggest variance between all mice. A simple example (Figure 5A and B) shows that a PCA can simplify data without losing much information (99.2% of data variance is represented in the 2D graph, Figure 5C and D), can help in recognizing differences between experimental groups, and offers loadings to potentially assign differences to certain parameters (Figure 5E). In this example, I could reduce dimensionality by one, which might not seem particularly powerful. In a real CatWalk experiment, like the one presented in this thesis, we can often reduce dimensionality from 200 to 2 without losing much information, where we go from unplottable data to an easily interpretable graph.

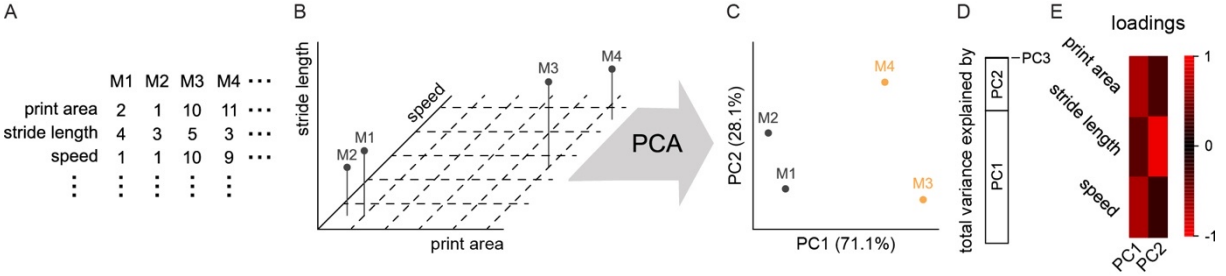

FIGURE 5 Example CatWalk data explaining PCA to reduce 3D to 2D datasets with marginal information loss. **(A)** Three CatWalk parameters from four mice. **(B)** Raw data is plottable in a 3D graph. **(C)** PCA allows for plotting the same data in a new 2D coordinate system with calculated PCs on the axes. Experimental groups differ in PC1 rather than PC2. **(D)** PCA induced limited information loss; total variance of the entire data set explained by the first two PCs is 99.2%. **(E)** Factor loadings explain how much a parameter correlates (values from -1 to 1) with a PC. Speed and print area correlate highly with PC1, which explains the biggest difference between the experimental groups.

TRACING STUDIES OF SPONTANEOUS REMODELING IN RODENTS AFTER TRAUMATIC SCI

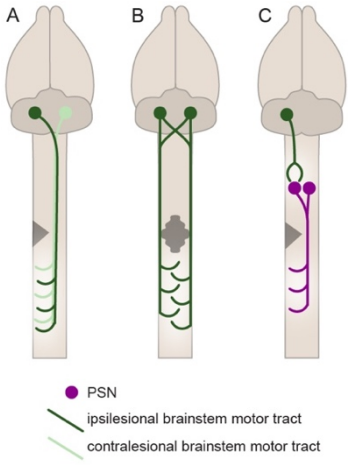

FIGURE 6 Remodeling involving brain stem motor tracts after SCI. **(A)** and **(B)** show the capacity of brain stem motor tracts to sprout. **(C)** Sprouting brain stem motor tracts can contact PSN, which sprout themselves to bridge the injury. Illustrations based on **(A)** ref. [111,118,119], **(B)** ref. [120], and **(C)** ref. [121,122].

The capacity of the CNS to compensate for the SCI induced loss of neuronal connections has been demonstrated in various settings, involving different populations of neurons. Remodeling, just like severity of SCI symptoms, depends on the location and completeness of the lesions. Motor tracts originating in the brain stem, such as the reticulospinal tract or vestibulospinal tract, have been shown to remodel in response to lateral hemisections. Fibers originating on the ipsilesional side bridge the lesion by crossing to the contralesional side rostrally, only to sprout back to the ipsilesional side below the lateral hemisection. [117,118] Similarly, fibers originating in the contralesional brain stem remain on that side of the spinal cord until beneath the lesion where they, then, also sprout to the ipsilesional side at various levels of the spinal cord (Figure 6A). [119] Even after severe contusions, where almost all of the spinal cord is damaged, spared fibers of the reticulospinal tract sprout below the injury (Figure 6B). [120] While these experiments prove that brain stem motor tracts are able to sprout, they do not investigate, which cells are contacted by the sprouting fibers. Just as in regeneration, extension of axonal length alone without contact formation does not generate crucial functional improvement.

To facilitate recovery, sprouting motor tracts must either contact denervated motoneurons directly or contact interneurons of the spinal cord, which in turn make connections with motoneurons. These interneurons belong to the category of propriospinal neurons (PSNs), which lie completely in the spinal cord, passing on information over short and long distances. After lateral hemisections, PSNs with a soma above the injury and spared projections traveling along the contralesional side have been shown to sprout to the ipsilesional side below the injury (Figure 6C). Killing these PSNs after they have remodeled eliminates behavioral recovery. [121] A subset of these PSNs with a soma on the ipsilesional side have been reported to receive increased input by brain stem motor pathways. [122] These studies indicate that PSNs are key players in successful remodeling after SCI. However, without identifying further connections to motoneurons, complete detour circuits with the ability to induce functional recovery remain undiscovered.

The CST and its capacity to remodel has long been at the center of chronic SCI research in rodents. Various experiments show the CST's capacity to sprout within weeks of the lesion inflicted. It was demonstrated that the ventromedial CST responds to a cervical injury of the dorsomedial CST by sprouting above the lesion and contacting motoneurons directly (Figure 7A). These new connections enable functional recovery in injured rodents. [123] Bareyre and colleagues extend the observation of remodeling to the ventrolateral CST. They show how injuring the major CST at a thoracic level leads to sprouting of both minor CSTs below the lesion where they contact motoneurons directly (Figure 7B). [110]

Thus, minor components of the CST can structurally and functionally take over the much more nominal dorsomedial component of the CST.

Consisting of a number of fibers far beyond the minor CST components, the dorsomedial CST's capacity to remodel is of particular interest. After a lateral hemisection, the fibers on the contralesional side have been shown to sprout to the ipsilesional side at various levels below the injury (Figure 7C). [124] Even when both sides of the major CST are injured, the hindlimb CST starts sprouting cervically (Figure 7D). [125,126]

Most detailed anatomical remodeling in rodents was characterized after a thoracic dorsal hemisection where an entire detour circuit could be traced, which reconnects a motor tract with its original, denervated motoneurons in the lumbar spinal cord via PSNs. As early as three weeks following injury, the hindlimb CST sprouts cervically to contact PSNs. A specific population of PSNs, long propriospinal neurons (LPSNs), are preferentially contacted, which project via the unlesioned ventral spinal cord to the lumbar region. These LPSNs, in turn, increase their contacts onto lumbar motoneurons (Figure 7E). [126] Relesioning the CST after remodeling took place reinstates early-injury motor deficiencies, highlighting the tract's role in functional recovery after SCI. Because of the detour circuit's uniquely detailed characterization, it offers wide opportunities to study remodeling mechanisms pertaining to sprouting and contact or synapse formation. Experiments described in this thesis make use of this detour circuit as an example to draw conclusions about general mechanisms of remodeling after SCI.

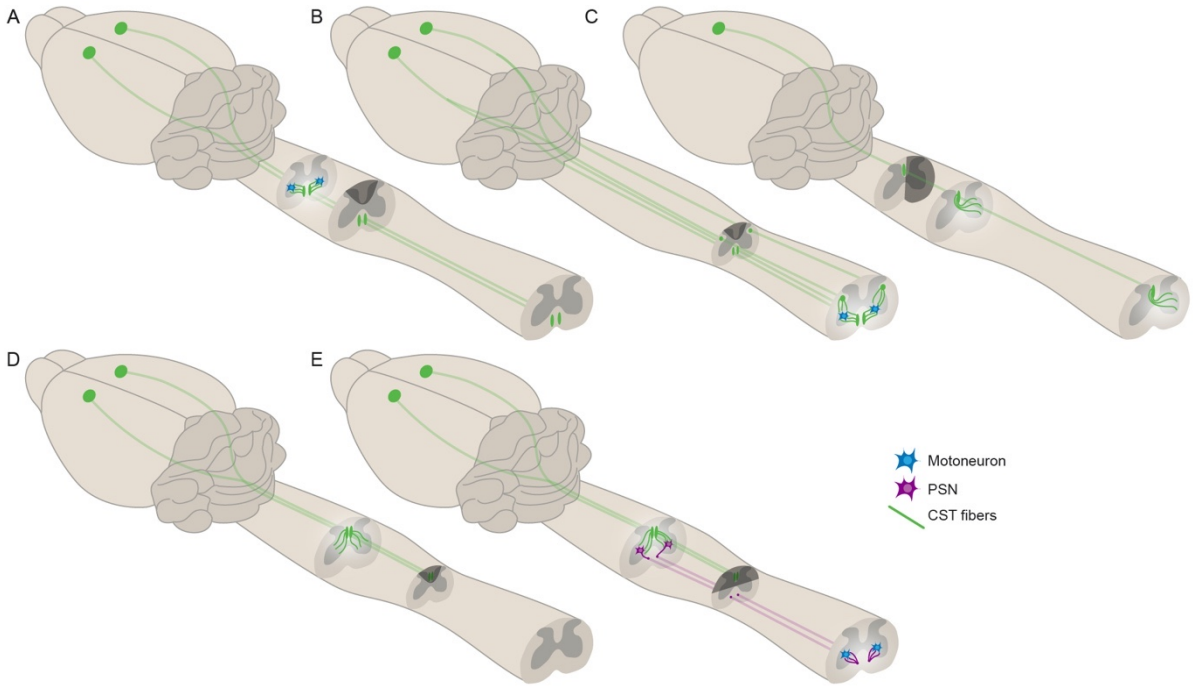

FIGURE 7 The CST exhibits robust remodeling capacities after SCI. **(A)** and **(B)** show the capacity of the minor CST components to remodel after injury to the major dorsomedial CST. **(C)** The dorsomedial CST sprouts to the unlesioned side after a unilateral hemisection. **(D)** and **(E)** the injured hindlimb dorsomedial CST sprouts above the lesion. **(E)** An entire CST detour circuit was identified after a thoracic dorsal hemisection. The hindlimb dorsomedial CST sprouts above the lesion to contact LPSNs, which sprout lumbarly to increase their projections onto motoneurons. Relesioning experiments show that this detour circuit is (partially) responsible for motor recovery after SCI. Due to its detailed description involving functionally relevant sprouting and contact formation, it is the basis for experiments presented in this thesis. Illustrations are based on **(A)** ref. [123], **(B)** ref. [110], **(C)** ref. [124], **(D)** ref. [125] and **(E)** ref. [126].

The rodent CNS' capacity to remodel spontaneously after SCI has been proven extensively. However, spontaneous remodeling does not lead to full functional recovery, yet. Research on interventions to support the already promising intrinsic capacity of the CNS to remodel after SCI is becoming increasingly popular. Aside from the aforementioned molecular interventions (targeting mTOR, KLF7, STAT3, chondroitin sulphate proteoglycans, and NogoA) that increase remodeling as well as regeneration, there are interventions that specifically target remodeling.

As previously described, rehabilitative training, like treadmill training, wheel running or pellet reaching, has been observed to improve motor functions in rodents. [107,108,127] This behavioral improvement was later attributed to increased sprouting of motor tracts above and below the lesion, [107,109,127] more directed sprouting to new areas of the spinal cord, [128] as well as increased contact formation between motor tracts and PSNs or motoneurons. [107] Increased remodeling after rehabilitation could be explained by altered gene expression profiles in areas of remodeling, inducing changes in growth factors, guidance molecules, and components of synaptogenesis. [128] Electrostimulation and pharmacological stimulation of areas with sprouting collaterals have also been shown to support remodeling. For example, positive effects of rehabilitative training can be further improved by combining it with epidural stimulation and serotonergic plus dopaminergic antagonists, both applied to remodeling supportive areas of the spinal cord. [120,129] Although this multifaceted approach has yielded, so far, maximal functional recovery, reaching levels of uninjured motor skills, that can be used at the rodent's own volition, can, still, not be accomplished.

OBJECTIVES

Optimizing interventions that target the CNS' already promising remodeling response is only possible if we completely understand the exact mechanisms underlying remodeling. Rehabilitative training, electrostimulation, and pharmacological stimulation, which specifically act on remodeling, rather than regeneration, all impact neuronal activity of certain spinal cord populations. In these setups neuronal activity was increased indiscriminately, disregarding neuronal populations. Moreover, anatomic analyses were limited to general changes to sprouting or contact formation.

Before publishing our paper in the Journal of Experimental Medicine, the exact role of neuronal activity in remodeling after SCI, however, remained to be elucidated. For the first time, we analyzed the importance of neuronal activity for CST remodeling after SCI in experiments, which will be presented and elaborated on in this thesis. [130]

To understand spontaneous remodeling, we decreased neuronal activity or activity dependent processes chronically in a well-known detour circuit after SCI (Figure 7E). After a thoracic dorsal hemisection, manipulations were performed in the spinal cord at the location of CST sprouting plus contact formation onto PSNs and entailed: (1) perturbing NMDAR transmission, (2) inhibiting the activity dependent cyclic AMP response element-binding protein (CREB) mediated transcription factor, and (3) directly suppressing neuronal activity using designer receptor exclusively activated by designer drugs (DREADDs).

Resulting changes to remodeling were quantified anatomically at the site of intervention, in terms of changes to CST collateral sprouting (by analyzing CST collaterals exiting the white matter to the gray matter and measuring total collateral length in the gray matter), collateral maturity (by analyzing bouton density along CST collaterals) and contact formation onto relay neurons. Functional remodeling was assessed using the aforementioned CatWalk experiment.

With this experimental setup our work elucidates the role of neuronal activity in detour circuit formation after SCI by answering the following questions:

1. How does perturbing NMDAR signaling, CREB function and neuronal activity in the spinal cord differentially affect detour circuits following injury?
2. Do these perturbations affect adult uninjured circuits and mature detour circuits, or is there a time sensitive window during which they exert their effects?
3. Do differences in levels of neuronal activity of cervical neurons impact target selection of remodeling CST fibers?
4. Is neuronal activity in the cervical spinal cord crucial for behavioral recovery following SCI?

We hypothesized that downregulating neuronal activity dependent processes in the mouse cervical spinal cord during remodeling affects the CST detour circuit when compared to nonmanipulated mice. The next two chapters are dedicated to our methodological setup and results obtained whilst pursuing the aforementioned objectives and testing our hypothesis.

MATERIAL AND METHODS

MOUSE STRAINS AND HUSBANDRY

Mice used in this thesis included: C57Bl/6 wildtype mice (Charles River, strain code#475), Vglut2-ires-cre (Jax#028863), [131] GlyT2-eGFP [132], and NR1^{flox} (Jax#005246) [133] mice. Vglut2-ires-cre mice express cre recombinase in all glutamatergic neurons without affecting endogenous expression of vesicular glutamate transporter 2. NR1^{flox} mice were used to create nonfunctional NMDAR by deleting the GluN1 subunit of the NMDAR when cre recombinase is expressed. GlyT2-eGFP express enhanced green fluorescent protein (eGFP) in all glycinergic cells without affecting endogenous expression of the glycine transporter 2.

All mice were between six and twelve weeks old at the beginning of experiments. Female mice were used preferentially. Mice were assigned randomly to control or experimental condition prior to injury. Experiments with mice of different age and sex were split equally between conditions although we observed no discernable difference in outcome based on age/sex.

If bred out of house, mice were given one week to adjust to the institution's animal facility before the start of experiments. Mice had access to food and water *ad libitum* and were housed in a light/dark cycle (12:12h). Animal care, including monitoring of weight, pain, and behavioral impairments, was performed twice daily for two weeks after injury and, as needed, until sacrifice. All animal experiments followed regulations of the animal welfare act and protocols approved by the district government of Upper Bavaria.

SURGICAL PROCEDURES

Exact timing of surgeries and assignment of type of surgery to each animal model are illustrated in the experimental setup scheme of each experiment's figure in the Results section. All surgeries were performed under full general anesthesia with a mixture of ketamin/xylazine (100 mg/kg ketamine and 13 mg/kg xylazine). Before surgery, mice were orally administered 15µl of meloxicam (Metacam, Boehringer Ingelheim, 2mg/kg) and kept on heating pads, at body temperature, until fully anesthetized as tested by a hindlimb toe pinch test. After surgery, mice were kept on heating pads until fully awake. There, they had *ad libitum* access to water and food and, in case they were spinally hemisected, received a 1ml subcutaneous injection of saline. 12h post-surgery mice again received 15µl of meloxicam. Meloxicam could be topped up 24h post-surgery, if the experimenter judged the mouse to still be in pain, based on facial expressions, grooming, food/water intake, vocalization of the mouse.

THORACIC DORSAL HEMISECTIONS

The mice' limbs were loosely pulled to the side with rubber bands. Incision into the skin at thoracic level was performed with a scalpel. Ribs and fat tissue aided in the identification of thoracic level 8 (T8). Incising into fat and muscle tissue exposed the T8 vertebra. A laminectomy was performed, and the

local anesthesia Lidocaine (Xylocaine 2% gel; AstraZeneca) was applied for 2min. With fine iridectomy scissors the spinal cord was dorsally hemisected, lesioning the major dorsomedial and minor dorsolateral CST, whilst leaving the minor ventromedial CST intact. Previously cut muscle tissue was sutured, and the skin was closed with wound clips.

STEREOTACTIC INJECTIONS

Injections were all performed with fine pulled glass micropipettes that were attached to syringes via cannulas. Micropipettes were slowly (0.1mm/min) lowered into the tissue using a stereotactic frame and remained at the final injection location for 1min before starting the injection. The tracer or AAV was injected slowly (~0.05µl/min) by applying weak syringe pressure to avoid tissue damage. After the injection was complete, the micropipette remained in place for another minute. Afterwards, it was extracted as slowly as it was inserted.

SPINAL CORD INJECTIONS

Mouse fixation, skin incision, and connective/muscle tissue removal were performed as described above. Cervical vertebrae were identified counting downward from cervical vertebra 1. Here, the dura was removed at injection site and AAV injected without a laminectomy. Where we injected twice cervically, we injected at cervical level 4 (C4; 0.5 µl AAV injected bilaterally, ±0.4mm lateral and -0.7mm depth). Where we injected four times to maximize expression in the behavioral and intersectional labeling experiments, we injected in an alternating pattern of right and left, spanning the spinal cord from C4 to C6 (2x0.5 µl AAV injected bilaterally; ±0.4mm lateral and -0.8mm depth).

Lumbar vertebrae were identified using ribs; the most caudal rib attaches to thoracic vertebra 13, lumbar vertebra 1 is caudal to this. Due to the small intervertebral space, a laminectomy was performed to expose the spinal cord at lumbar level 1. 0.5µl AAV/Fluorogold (1% in 0.1M Cacodylate buffer, Fluorochrome) were injected bilaterally at ±0.3mm distance to the midline and -0.6mm depth. After spinal cord injections, mice were closed up as described above.

BRAIN INJECTIONS

For brain injections, the mouse head was fixed in a stereotactic frame. The skin was incised with a scalpel roughly above the motor cortex. Using bregma, injection coordinates were determined on top of the skull, and holes in the bone were created with a dental drill. 1µl BDA (10000MW, Life technologies, dissolved in 0.1M phosphate buffer) was injected bilaterally (hindlimb motor cortex coordinates from bregma: −1.3mm caudal, ±1.2mm lateral, and -0.6mm depth; forelimb motor cortex coordinates from bregma: −0.6mm caudal, ±1mm lateral, and -0.6mm depth). The skin was closed with wound clips.

NEURONAL ACTIVITY MANIPULATION

Exact timing of manipulations and assignment of specific AAV to each animal model are illustrated in the experimental setup scheme of each experiment’s figure in the Results section.

AAV TOOLS

The control pAAV-CMV-GFP was created by inserting an eGFP sequence from pEGFP-N1 (Clontech) into the HincII site of pAAV-CMV-MCS (Stratagene). For pAAV-CMV-GFP-Ires2-Cre the following sequences were inserted additionally, upstream of GFP in the order of: cre sequence from Cre-recombinase expression vector pBS185 (gift from Thomas Hughes, Montana State University), ires sequence from pIres2-DsRed2 (BD Bioscience). pAAV-CMV-eGFP-T2A-aCREB was gifted from H. Gainer (National Institute of Neurological Disorders and Stroke, National Institutes of Health, Bethesda, MD). pAAV-hSyn-DIO-hM4D(Gi)-mCherry was a gift from B. Roth (University of North Carolina, Chapel Hill, Chapel Hill, NC).

We followed standard procedure to generate AAVs with the aforementioned plasmids at a 1:1 ratio of AAV1 and AAV2 capsid proteins. All remaining AAVs used were purchased from addgene: AAV2-hSyn-DIO-hM4Di(Gi)-mCherry (catalog#44362-AAV2), AAV8-hSyn-DIO-hM4Di(Gi)-mCherry (catalog#44362-AAV8), and AAV2-pmSyn1-eBFP-cre (catalog#51507-AAVrg). All AAV plasmids are allocated to the respective experiments in Table 1. All genomic titers exceeded 1x10e10.

Manipulation	Figure	Plasmid	Promoter
NR1 experiment	13C-F, 19A-B	pAAV-CMV-eGFP	CMV
		pAAV-CMV-eGFP-IRES-Cre	CMV
	15	pAAV-CMV-eGFP	CMV
		pAAV-CMV-eGFP-IRES-Cre	CMV
CREB experiment	14, 19C-9	pAAV-CMV-eGFP	CMV
		pAAV-CMV-eGFP-T2A-aCREB	CMV
	16	pAAV-CMV-eGFP	CMV
		pAAV-CMV-eGFP-T2A-aCREB	CMV
Global silencing	17A-D, 19E (top), 19F (left)	pAAV-CMV-eGFP-IRES-Cre	CMV
		pAAV-hSyn-DIO-hM4D(Gi)-mCherry	hSyn
Selective silencing	17E-M, 19E (bottom), 19F (right)	pAAV-hSyn-DIO-hM4D(Gi)-mCherry	hSyn
	18	pAAV-hSyn-DIO-hM4D(Gi)-mCherry	hSyn
LPSN silencing	17N-P	pAAV-pmSyn1-eBFP-cre	pmSyn1
		pAAV-hSyn-DIO-hM4D(Gi)-mCherry	hSyn

TABLE 1 AAV plasmids used in respective experiments of this dissertation.

PHARMACOLOGICAL MANIPULATION

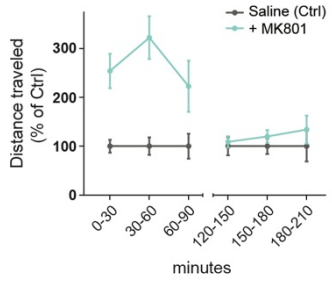

FIGURE 8 MK801 injection does not lead to movement decline. Distance traveled after 0.25mg/kg MK801 or saline injection in an open field setup. Each time point was measured in 30min intervals. Bar lengths represent means, and error bars represent SEMs. One independent experiment (n = 4 mice per experimental setting).

To block NMDAR pharmacologically, animals received a daily i.p. injection of MK801 (0.25mg/kg in saline, Tocris Bioscience). The dose was based on a previous, developmental study. [134] We ruled out that a reduction in anatomical remodeling was indirectly caused by a decline in locomotor activity due to MK801 administration. The movement of mice after MK801 injection was tracked in an open field for up to 3h. MK801 did not induce sedation but a transient increase in locomotor activity (Figure 8).

To stimulate DREADDs, the hM4Di receptor specifically, and decrease neuronal activity, we administered subcutaneous clozapine-N-oxide (CNO; 1mg/kg diluted in saline, Sigma-Aldrich) every 12h. Before behavioral testing, animals were not treated with CNO for 24h to ensure

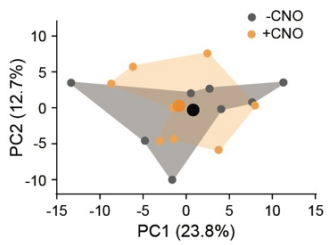

FIGURE 9 Chronic CNO administration alone does not lead to chronic behavioral effects. Mice were lesioned and, starting at 14dpi, treated with twice daily injections of CNO (1mg/kg, orange) or saline (black) until 21dpi. One day after the last injection locomotion was tested using CatWalk. No differences after PCA on CatWalk parameters could be seen between the saline-treated and the CNO-treated group. Small dots represent each mouse, big dots represent the mean of each group. One independent experiment (n = 7-8 mice per experimental setting).

that observations were based on chronic anatomic changes and not on transient silencing of neurons. We did not observe significant behavioral effects from chronic CNO administration alone (Figure 9). Instead of MK801 and CNO, controls received saline with the same respective administration scheme as described above.

TISSUE PROCESSING

TRANSCARDIAL PERFUSION

Mice were sacrificed by isoflurane overdose (AbbVie, North Chicago, US) and perfused intracardially with 4% paraformaldehyde in phosphate buffered saline (PBS). After extracting skull and vertebral column from the mouse body, the tissue was stored in the perfusion solution for 24h. Tissue was rinsed in PBS before microdissecting, i.e. removing the intact spinal cord and brain from vertebrae and skull. Spinal cord and brain were, then, transferred to 30% sucrose in PBS for 48h cryoprotection.

CUTTING

Freezing the tissue in optimal cutting temperature medium (Tissue-Tek, Sakura, Finetek, USA) for at least 20min prepared it for cryostat (Leica CM1850) cutting. We cut 50µm coronal sections of the cervical enlargement and brain containing motor cortex as well as sagittal sections of the lesioned thoracic spinal cord. The cervical spinal cord was cut free-floating and only mounted after staining, creating a random order of sections. After cutting the thoracic spinal cord and brain sections, they were directly and sequentially mounted on slides coated in 0.5% gelatin and 0.05% chromium potassium sulfate.

STAINING

To amplify the BDA signal, sections were incubated with the ABC Complex (Vector Laboratories) overnight at 4°C. After a tyramide amplification (Biotin-XX, TSA Kit 21, Life Technologies) for 30min, sections were incubated in streptavidin-conjugated Alexa Fluor 647 (1:500 in PBS, Life Technologies) or streptavidin-conjugated Alexa Fluor 594 (1:500 in PBS, Life Technologies) overnight.

AAV induced expression was amplified with immunohistochemistry when the virus was only expressed for seven days. AAVs with mCherry yielded dotty labeling. Hence, NeuN staining was performed to determine the boundaries of the infected neurons. Synapsin-I staining aided in the characterization of bouton maturity (explained in “Image Acquisition, Processing and Analysis”). Before applying antibodies, all sections were treated with a blocking solution (10% goat serum/0.1% TritonX/PBS) for 1h at room temperature. All subsequent antibody stainings are summarized in Table 2. All samples were coverslipped with Vectashield (Vector Laboratories).

Primary Antibody	Incubation	Secondary Antibody	Incubation
rabbit anti-GFP (1:500, A11122, Life Technologies)	4°C, overnight	goat anti-rabbit-488 (1:500, A11008, Life Technologies)	4°C, overnight
rabbit anti-Synapsin-I (1:500, AB1543, Millipore)	4°C, 24h	donkey anti-rabbit-DyLight 405 (1:100, AB_2340616, Jackson Immunoresearch)	room temperature, 6h
mouse anti-NeuN antibody (1:500, MAB377, Millipore)	4°C, overnight	goat anti-mouse-488 (1:500, A11001, Life Technologies)	4°C, overnight

TABLE 2 Protocols for immunohistochemical staining used in this dissertation.

IMAGE ACQUISITION, PROCESSING, AND ANALYSIS

For figures of this thesis, images of boutons (20x objective, 1024 × 1024 pixels, zoom x1.1, 0.45µm z-resolution, Kalman integration: 2), and the overview image of LPSN infection (20x objective, 1024 x 1024 pixels, zoom x1, 0.45µm z-resolution) were scanned at high resolution with an Olympus FV1000 confocal microscope. The LPSN overview image was stitched in Fiji with the plugin "Grid/Collection". To reduce background fluorescence from lipofuscin and spectral overlap in the AAV channel, we subtracted the BDA channel from it. For illustration purposes, some images were subjected to gamma adjustments in Fiji or Adobe Photoshop.

Acquisition settings for illustration purposes and analysis of all images were the same for the experimental and control group of one experiment. The experimenter was blinded for image analyses concerning experimental and control group.

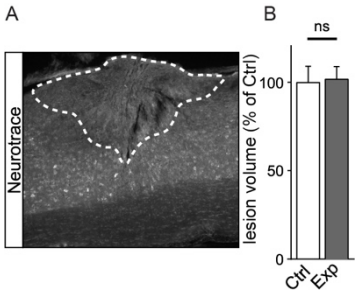

FIGURE 10 Mice received reproducible thoracic dorsal hemisections. **(A)** Sagittal section at T8 of example lesion, dotted line indicates lesion measurement in single images. **(B)** Lesion volumes of mice analyzed did not differ between control and experimental groups (p = 0.1121). Data analyzed using student's t test (two-tailed, unpaired). Bar lengths represent means, and error bars represent SEMs. Scale bar: 100µm. ns: not significant. Nine grouped independent experiments (n = 29-39 mice per experimental condition).

LESION VOLUME

Neurotrace stained sections with lesion were scanned using an Olympus IX71 fluorescence microscope (5x objective, 1376x1032, zoom x1). Resulting 2D images were processed with ImageJ, and the lesion area was identified based on the integrity of neurotrace stained neurons. Both, the cavity and surrounding damaged tissue, was outlined (Figure 10A). To quantify the lesion volume, the measured lesion area of each section was multiplied by the section thickness (50µm), and the results of consecutive sections were summed for each animal to provide a final estimation of the total lesion volume. No significant difference between experimental and control groups could be detected (Figure 10B), illustrating the reproducibility of dorsal hemisections induced by the experimenters.

LOCALIZATION OF AAV+ NEURONS

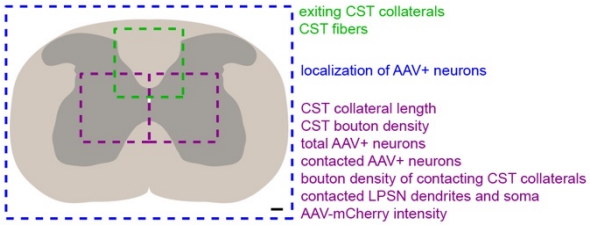

FIGURE 11 Different fields of view for analyses on sections of the cervical enlargement. Scale bar: 100µm.

Low resolution images of 4 whole spinal cord sections per animal (Figure 11) were acquired with an upright Leica DM4 fluorescence microscope (5x objective, 1392x1040 pixels, zoom x1). Images were registered on an Adobe photoshop template so that all sections were oriented the same with the central canal in the same position. For illustration purposes, the coordinates of registered neurons were then extracted from Fiji and used to create topographic maps in Python, which in turn were placed on a spinal cord template from a mouse spinal cord atlas. [12]

RULING OUT UNDESIREABLE RETROGRADE AAV INFECTION

To ensure that AAV manipulation only occurred in the spinal cord and did not affect CST fibers by undesirable retrograde transport of the virus, we analyzed the motor cortex for any AAV-induced fluorophore positivity. At least three brains (from 300µm rostral to 300µm caudal of BDA injection site) per experimental group were checked under an Olympus IX71 fluorescent microscope and no AAV positive cells could be detected.

CST FIBERS

To control for differences in BDA labeling, all quantifications involving the CST were normalized to the number of BDA-labeled fibers quantified in the dorsomedial CST. CST labeling inside the dorsal column of the cervical tract was relatively uniform, so that an analysis of 3-5 sections in this area was representative of BDA labeling in the entire animal. Per animal, the first 6µm of at least 3 random dorsal columns were scanned (Figure 11) using an Olympus FV1000 confocal microscope (20x objective, 640 × 640 pixels, zoom x1.1, 0.45µm z-resolution). Images where long CST collaterals crossed the tract were excluded from the analysis. Images were analyzed in an automated fashion: The “Analyze Tubeness” Fiji plugin was applied to the tract. The number of fibers were, then, quantified using the “3D Object Counter” plugin.

EXITING CST COLLATERALS

Exiting collaterals were quantified on images (Figure 11) of at least 30 sections taken with an Olympus FV1000 confocal microscope (20x objective, 640 × 640 pixels, zoom x1.1, 0.45µm z-resolution) in Imaris. In case of hindlimb CST tracing the entire depth of the dorsal column in a section was analyzed. Where forelimb CST fibers were traced, labeling was so dense that only the upper 5µm of each section were quantified. In Imaris, in 3D “blend mode”, all collaterals clearly crossing the gray/white matter boarder were manually counted. The total number of exiting collaterals per animal was normalized to the respective number of BDA labeled CST fibers.

MAIN GRAY MATTER ANALYSES

Per animal, at least 20 sections were scanned using an Olympus FV1000 confocal microscope (20x objective, 640×640pixels, zoom x1.1, 0.45µm z-resolution). Instead of scanning and stitching entire sections, one image was acquired left and right of the spinal cord midline. Image field of views were positioned with the midline and central canal as reference points – the midline aligned with the right or left edge of the image, and the central canal is positioned one third from the top (Figure 11). This position allowed for two separate images covering the vast majority of gray matter where CST sprouting occurred. Few images from animals with injections of AAVs with a CMV promoter, were excluded from the analysis if glial cells were labeled as assessed by their different morphology as opposed to neurons. In the following, all analyses on the described images will be outlined.

CST COLLATERAL LENGTH

On converted 8bit, maximum intensity z projections, collaterals were traced semi-automatically using the “NeuronJ” Fiji plugin. Length of all collaterals was summed up per section and normalized to the respective number of BDA labeled CST fibers.

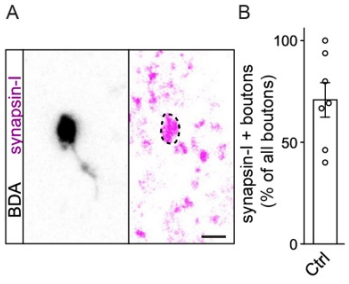

FIGURE 12 The majority of identified boutons are synapsin-I positive. **(A)** Example bouton with synapsin-I staining. Left: confocal maximum projection of BDA labeled CST collateral, right: single plane synapsin-I staining at center of bouton. Dotted line indicates bouton border. **(B)** Quantification of synapsin-I staining in more than 80 boutons. Bar length represents mean, and error bar represents SEM. Scale bar: 2µm. One independent experiment (n = 6 mice).

CST BOUTON DENSITY

On maximum z projections, experimenters were trained to recognize boutons on CST collaterals based on size and brightness in relation to immediately adjacent collaterals. More precisely, the bouton’s maximum Ferret diameter needed to be ~2x bigger and its maximum intensity ~3x brighter. Bouton density was, then, calculated by dividing bouton number by collateral length per image.

In a subset of recognized boutons (n = 122), we confirmed that experimenters adhered to the aforementioned criteria. Furthermore, we consider the majority of identified boutons as mature since they already express presynaptic machinery attested by synapsin-I staining. In rescanned high-resolution images with a Leica TCS SP8 confocal microscope (63x objective, 788x788pixels, zoom x1, 0.3µm z-resolution), above 70% of boutons were considered synapsin-I positive (Figure 12).

TOTAL AAV+ NEURONS

To control for differences in AAV expression, all quantifications involving AAV infected neurons were normalized to the number of these cells. For this purpose, number of AAV positive cells were counted manually on maximum intensity projections.

CONTACTED AAV+ NEURONS

It was sufficient to analyze 10 of the scanned sections per animal for contacted AAV positive neurons. In case of hindlimb CST labeling, the entire image stack was assessed, and for dense forelimb

CST labeling only 5µm of each section were analyzed. AAV positive contacted neurons were analyzed in 3D “blend mode” in Imaris. For AAV-mCherrys, contacts were analyzed on NeuN stained neurons and later checked for AAV positivity (described below). For AAV-GFPs, a median filter was applied to the GFP channel to bring cell bodies and proximal rather than distal dendrites infected to the foreground. This reduced the complexity of an image and allowed us to assign dendritic contacts to a specific neuron.

If the following criteria were met, contacted cells were counted: (1) due to point spread of confocal images, a CST collateral needed to clearly overlap with the cell body or a proximal dendrite, (2) collaterals exhibited a bouton (meeting additional criteria as described above) where they touched the AAV infected cell. In Imaris, contacted neurons were marked with the “measurement points” tool. The total number of contacted cells per section was normalized to the respective number of BDA labeled CST fibers of an animal and the number of AAV infected neurons of the same section.

To verify our approach of analyzing contacted neurons, we rescanned a subset of them (n = 137 of 7 animals) at high resolution using an Olympus FV1000 confocal microscope (20x objective, 1024x1024pixels, zoom x7.7, 0.15µm z-resolution) and reanalyzed them on single planes in Fiji. All of the contacted cells recognized with lower resolution in 3D were reidentified as contacts in 2D high resolution images.

BOUTON DENSITY OF CONTACTING CST COLLATERALS

In one experiment we not only measured the number of contacted AAV neurons but also how many boutons were in close apposition with one contacted neuron. In addition, we normalized the number of boutons to a measured length of a stretch of CST collateral that clearly overlapped with an AAV infected cell, yielding a measurement of bouton density of collaterals contacting AAV positive neurons.

CONTACTED LPSN DENDRITES AND SOMA

In our sparsely labeled LPSN experiment, we could investigate whether manipulation would affect contacts onto somata and proximal or distal dendrites differentially. This analysis was performed in Fiji where potential contacts were first identified on maximum projections and afterwards confirmed or refuted on single planes using the same criteria as described above.

AAV-MCHERRY INTENSITY

DREADD receptor coupled mCherry intensity inside NeuN positive neurons was determined in Imaris. The surfaces of NeuN neurons were rendered using the “Marching cubes” setting in the Imaris “Surface” tool. Mean mCherry intensities per analyzed neuron were extracted. Background mean intensity was measured in selected regions of interest devoid of AAV positive structures on five average-intensity projections per mouse in Fiji. Averaged gray matter background mCherry intensity was subtracted from neuronal mCherry intensities. If the neuronal intensity was higher than the mean background intensity, the NeuN cell was considered mCherry positive.

MOTOR SKILL ANALYSIS

Motor skills were assessed with a CatWalk XT (Noldus) system. The pre-injury mice were habituated to the setup three times, one week prior to the first recording. At each time point, three successful runs were recorded per mouse that followed the preset requirements, based on recommendations by the manufacturer: (1) minimum run duration of 0.5s, (2) maximum run duration of 4s, (3) maximum speed variation of 60%. These requirements guaranteed a low variance in between runs. All runs were, thus, comparable, and the different parameters could be analyzed across mice and treatment groups. As in previous studies, recordings always took place one day after the last CNO/saline injection. [135] This setup ensured that short-term CNO or its metabolized form would not affect the mice' behavior by actively silencing DREADD infected cells. All behavioral changes observed could, thus, be explained by anatomic long-term alterations.

CatWalk generated 177 parameters. To interpret the data, we performed a PCA with the online tool ClustVis (row scaling: "unit variance scaling", PCA method: "SVD with imputation") [136] on the 21dpi data, as this was our time point of interest. We applied the generated 21dpi parameter loadings and the unit variance scaling to the other time points to calculate each mouse' value for principal component (PC) 1 and 2. We used the pre-injury PC1 of each mouse as a baseline and subtracted it from PC1 values at other time points to reduce between mice variance not explained by CNO treatment (Figure 18D). To show that chronic CNO administration alone does not alter locomotion after SCI we repeated the same motor skill analysis (Figure 9).

MK801 motoric data to exclude the possibility of sedative effects of the drug (Figure 8) were generated in an open field. The mice' movement was tracked in 30min intervals using the automated tracking software ANY-maze (v. 4.99). To reduce stress in animals, 0-90min and 120-210min were tested on different days.

STATISTICS

For ease of illustration and to combine sets of experiments acquired at different time points, data sets are expressed as percentages of controls. All statistical evaluations were performed in GraphPad Prism (v. 7.00). Normality was tested using D'Agostino-Pearson omnibus normality test. When data were normally distributed, control and experimental groups were compared using an unpaired, two-tailed student's t test and data were normalized to the control mean. Results are, then, reported as mean ± SEM. When data did not pass the normality test, control and experimental groups were compared using Mann-Whitney (Figure 17K right, Figure 17M right) or Kolmogorov-Smirnov test (Figure 17K left), and data were normalized to the control median. The medians of data analyzed with a Mann-Whitney test are presented in box-and-whisker plots, where box borders represent the 25^{th} and 75^{th} percentile and whiskers the 10^{th} and 90^{th} percentile. Data analyzed with a Kolmogorov-Smirnov test are presented in cumulative frequency graphs with the upper limit set to 100% of the experimental group. Behavioral data with multiple time points (Figure 18D) were evaluated with a repeated two-way ANOVA. Primary measure showed statistical significance and was, thus, followed by a Bonferroni post hoc t-test.

Statistical outliers were determined with the robust regression and outlier test (Q = 1). Only four animals were detected and excluded from all analyses. Significance level is defined as follows: *$p < 0.05$, **$p < 0.01$, ***$p < 0.001$, and ****$p < 0.0001$.

RESULTS

MANIPULATING NMDAR FUNCTION ALTERS CST REMODELING

To first probe our hypothesis of neuronal activity playing a role in CST remodeling after SCI, we pharmacologically inhibited NMDARs with the antagonist MK801. In unmodified, spontaneous remodeling three weeks after a thoracic dorsal hemisection, rodent CST fibers will have sprouted extensively in the cervical enlargement to contact PSNs. [126] We, thus, examined the effects repeated MK801 injections would have during detour circuit establishment (2-3weeks after injury) on the remodeling of CST collaterals in the cervical enlargement (Figure 13A). We quantified *en passant* boutons on BDA labeled CST collaterals in confocal images of the cervical spinal cord. Boutons represent presynaptic swellings that typically contain synaptic vesicles and an active zone. [137] The number of boutons was normalized to CST collateral length, to ensure that a change in bouton number did not result from a mere reduction in collateral length. Pharmacologically blocking NMDARs with MK801 led to a significant decrease in bouton density of CST collaterals when compared to control mice treated with saline (Figure 13B).

An antagonist like MK801 binds to all NMDARs in the murine CNS. Thus, the observed reduction in bouton density could be explained by NMDAR blocking in the cortex as the origin of the remodeling CST itself, by NDMAR blocking in spinal target neurons of the remodeling CST, or by other off-target effects. To restrict NMDAR manipulation to the location of CST sprouting plus contact formation onto PSNs, we performed spinal cord anterograde AAV injections at C4 of an NR1 floxed mouse line (Figure 13C). In this mouse line, the sequence for NR1, a subunit of the NMDAR, is flanked by lox sites. Upon expression of cre, induced by an AAV-GFP-cre injection, the NR1 sequence is excised, rendering the receptor nonfunctional in cervical neurons. Control mice received C4 injections with an AAV lacking the cre sequence. Adjusting the titers of both AAVs led to similar GFP expression in terms of the number of infected cells (AAV-GFP-Cre: 147 ± 13 GFP positive neurons/section, AAV-GFP: 167 ± 8 GFP positive neurons/section; n = 6-8 mice per group) and their localization (Figure 19B).

Similar to pharmacological blocking of NMDARs, this manipulation during detour circuit development led to a decrease in bouton density along sprouting CST collaterals (Figure 13E). While boutons have long been accepted to functionally connect neurons, they merely represent the presynaptic structure. Thus, bouton analysis alone does not explain which spinal neurons are contacted less. We extended our analysis to assess whether these presynaptic CST boutons are less likely to contact NMDAR manipulated neurons, tagged with GFP. In fact, knocking out NMDAR during detour circuit establishment significantly decreased the number of contacted GFP positive neurons in comparison to control, NMDAR competent, mice (Figure 13D). NMDAR function, thus, appears to be crucial in the formation of contacts between motor tract collaterals and relay neurons of detour circuits. Other than synaptic impairments, general CST collateral anatomy in the cervical cord, such as the total

collateral length in the gray matter or the number of collaterals exiting the white matter tract to enter gray matter, remained unaltered (Figure 13F and 19A).

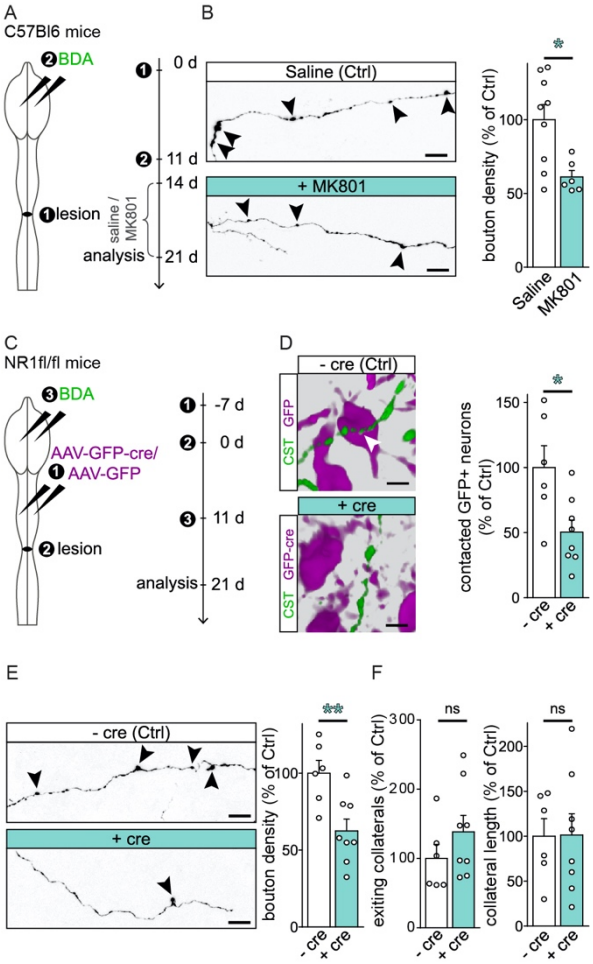

FIGURE 13 Manipulating NMDAR function alters CST remodeling. **(A)** Experimental setup for pharmacological inhibition of NMDARs during detour circuit formation after a thoracic dorsal hemisection. **(B)** Left: confocal maximum projection of exemplary CST collaterals in the cervical gray matter with bouton quantification indicated with arrows. Right: quantification of bouton density (number of boutons per collateral length) along CST collaterals in NMDAR inhibited (MK801) versus non-inhibited mice (Saline; p = 0.0113). **(C)** Experimental setup for genetically inhibiting NMDAR function in cervical neurons during detour circuit formation after a thoracic dorsal hemisection. **(D)** Left: 3D reconstruction of an example confocal image showing the analysis of contacted GFP+ neurons. A contact is indicated with an arrow, which identifies the GFP+ neuron as contacted. Right: quantification of the number of contacted GFP+ neurons in mice with NMDAR functioning (-cre) versus nonfunctioning (+cre) cervical neurons (p = 0.0168). Values are normalized to the number of GFP+ neurons and CST labeling (assessed by number of BDA labeled CST white matter fibers). **(E)** Left: confocal maximum projection of exemplary CST collaterals in the cervical gray matter with bouton quantification indicated with arrows. Right: quantification of bouton density along cervical CST collaterals (p = 0.0064) **(F)** Left: quantification of the number of cervical CST collaterals exiting the white matter to enter the gray matter (p = 0.2584). Right: quantification of the total length of all CST collaterals in the cervical gray matter (p = 0.9673). Values are normalized to CST labeling. Data analyzed using student's t test (two-tailed, unpaired). Bar lengths represent means, and error bars represent SEMs. *p < 0.05, **p < 0.01. Scale bars, 10µm in (B), (D), and (E). Ctrl: control. ns: not significant. (B) one experiment (n = 6-9 mice per group) with experimental setup shown in (A); (D)–(F) two grouped independent experiments (n = 6-8 mice per experimental condition) with experimental setup shown in (C). Figure adapted, with permission from ref. [130].

MANIPULATING CREB FUNCTION ALTERS CST REMODELING

To investigate whether pathways downstream of NMDAR signaling play a role in CST remodeling after SCI, we inhibited the activity dependent transcription factor CREB. For this purpose, we made use of aCREB, a mutated version of CREB, which prevents binding of endogenous CREB to the DNA. For the experimental condition, we injected an anterograde AAV-GFP-aCREB into C4 of wildtype C57Bl6 mice and compared their CST remodeling to control mice with mere anterograde AAV-GFP injections (Figure 14A). Both AAVs exhibited similar spinal cord infection, quantified by the number of infected cells (AAV-GFP-aCREB: 159 ± 8 GFP positive neurons/section, AAV-GFP: 148 ± 8 GFP positive neurons/section; n = 6-8 mice per group) and their location (Figure 19D).

Similar to NMDAR manipulation, inhibiting CREB during detour circuit formation resulted in a decrease in the number of manipulated spinal neurons contacted by CST collateral boutons (Figure 14B). The most prominent change occurred in CST collaterals themselves. CREB inhibition after SCI

caused a decrease in the number of CST collaterals entering the cervical gray matter (Figure 14D and 19C) and in their total length (Figure 14E). Innervation of the cervical gray matter was, thus, significantly sparser. These shorter CST collaterals did not exhibit a reduction in bouton density (Figure 14C).

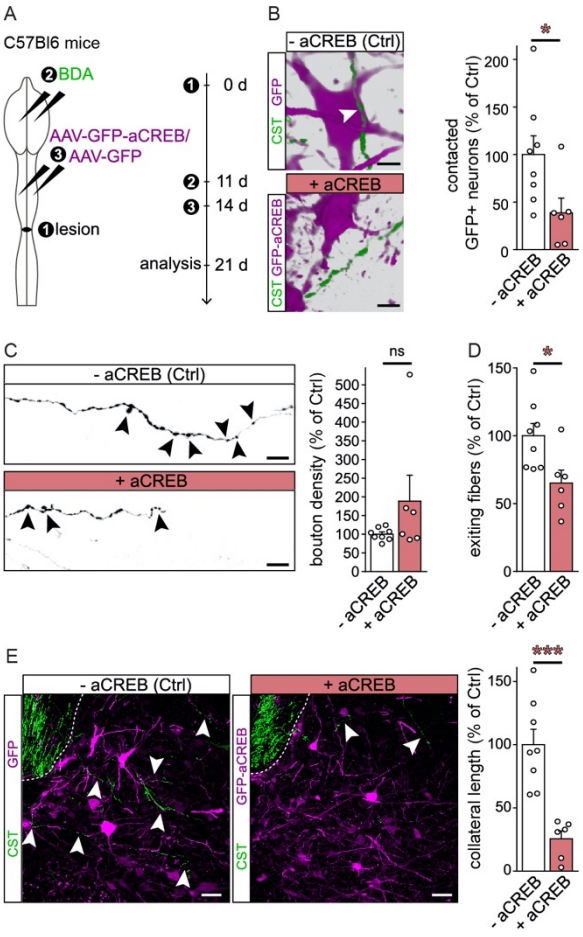

FIGURE 14 Manipulating CREB function alters CST remodeling. **(A)** Experimental setup for genetically inhibiting the activity dependent transcription factor CREB during detour circuit formation in cervical neurons after a thoracic dorsal hemisection. **(B)** Left: 3D reconstruction of an example confocal image showing the analysis of contacted GFP+ neurons. A contact is indicated with an arrow, which identifies the GFP+ neuron as contacted. Right: quantification of the number of contacted GFP+ neurons in mice with CREB operational (-aCREB) versus inhibited (+aCREB) cervical neurons ($p = 0.0393$). Values are normalized to the number of GFP+ neurons and CST labeling. **(C)** Left: confocal maximum projection of exemplary CST collaterals in the cervical gray matter with bouton quantification indicated with arrows. Right: quantification of bouton density along cervical CST collaterals ($p = 0.1636$). **(D)** Quantification of the number of cervical CST collaterals exiting the white matter to enter the gray matter ($p = 0.0229$). Values are normalized to CST labeling. **(E)** Left: confocal maximum projection of exemplary cervical gray matter area where CST sprouting occurs. Arrows indicate collaterals. Dotted line indicates white matter border. Right: quantification of the total length of all CST collaterals in the cervical gray matter ($p = 0.0004$). Values are normalized to CST labeling. Data analyzed using student's t test (two-tailed, unpaired. Bar lengths represent means, and error bars represent SEMs. *$p < 0.05$, ***$p < 0.001$. Scale bars, 10µm in (B) and (C); 50µm in (E). Ctrl: control. ns: not significant. Two grouped independent experiments (n = 6-8 mice per experimental condition) with experimental setup shown in (A). Figure adapted, with permission from ref. [130].

MANIPULATING ACTIVITY DEPENDENT PROCESSES IN MATURE CIRCUITS DOES NOT ALTER CST ANATOMY

To test whether manipulating activity dependent processes impacts mature circuits, we genetically perturbed NMDAR function after a functioning detour circuit had already been established, i.e. 12 weeks after SCI (Figure 15A). Contrary to manipulating NMDAR function during detour circuit establishment, a delayed manipulation of spinal neurons did not affect CST anatomy in the cervical spinal cord. More specifically, the number of GFP positive contacted neurons (Figure 15B), bouton density along CST collaterals (Figure 15C), CST collateral length, and the number of exiting CST collaterals (Figure 15D) were unaltered.

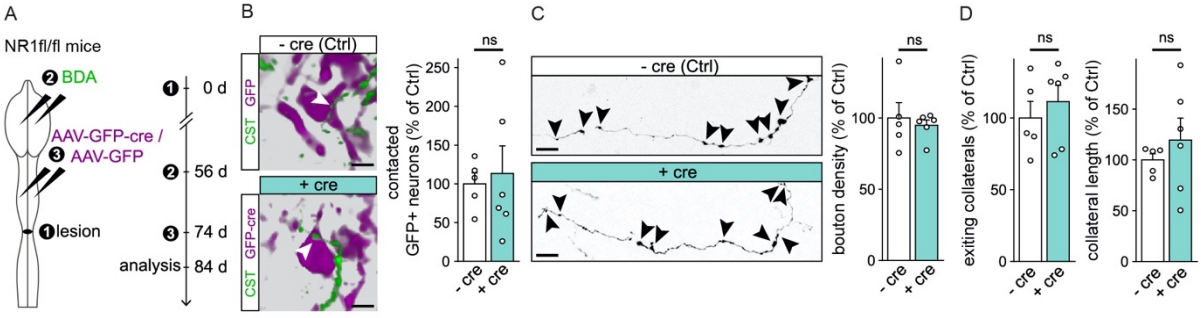

FIGURE 15 Manipulating NMDAR function in a mature detour circuit does not alter CST remodeling. **(A)** Experimental setup for pharmacological inhibition of NMDARs in cervical neurons after detour circuit formation following a thoracic dorsal hemisection. **(B)** Left: 3D reconstruction of an example confocal image showing the analysis of contacted GFP+ neurons. A contact is indicated with an arrow, which identifies the GFP+ neuron as contacted. Right: quantification of the number of contacted GFP+ neurons in mice with NMDAR functioning (-cre) versus nonfunctioning (+cre) cervical neurons (p = 0.7564). Values are normalized to the number of GFP+ neurons and CST labeling. **(C)** Left: confocal maximum projection of exemplary CST collaterals in the cervical gray matter with bouton quantification indicated with arrows. Right: quantification of bouton density along cervical CST collaterals (p = 0.6397). **(D)** Left: quantification of the number of cervical CST collaterals exiting the white matter to enter the gray matter (p = 0.5023). Right: quantification of the total length of all CST collaterals in the cervical gray matter (p = 0.4458). Values are normalized to CST labeling. Data analyzed using student's t test (two-tailed, unpaired). Bar lengths represent means, and error bars represent SEMs. Scale bars, 10µm in (B) and (C). Ctrl: control. ns: not significant. One experiment (n = 5-6 mice per experimental condition) with experimental setup shown in (A). Figure adapted, with permission from ref. [130].

To answer whether CREB could influence mature, intact neural circuits, we genetically inhibited the transcription factor as described above, but without a lesion and with a traced forelimb rather than hindlimb CST (Figure 16A). In the mature and intact CNS, forelimb CST fibers have numerous connections with spinal neurons in the cervical cord to generate movement of the forelimbs. Manipulating CREB in these spinal neurons did not induce any detectable anatomic alterations. Forelimb CST collateral boutons contacted a similar number of CREB deficient and competent (GFP positive) neurons in the cervical cord of control and experimental mice (Figure 16B). Its CST collateral morphology was unaltered in terms of bouton density (Figure 16C), number of exiting collaterals (Figure 16D) and total collateral length (Figure 16E). Manipulating NMDAR and CREB function by itself, thus, does not alter anatomic circuits, but its effects are specific to phases of detour circuit formation.

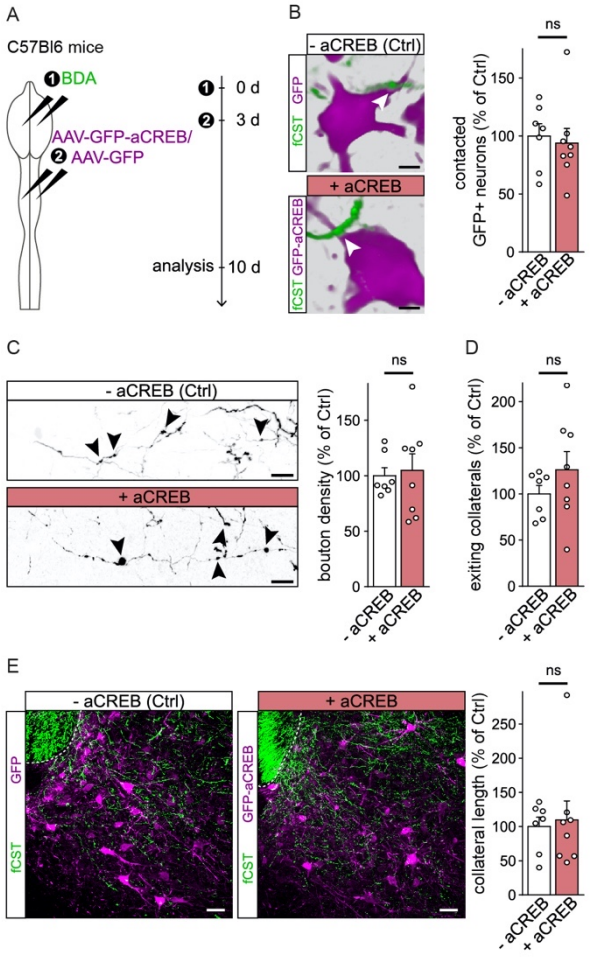

FIGURE 16 Manipulating CREB function in a mature circuit does not alter CST anatomy. **(A)** Experimental setup for genetically inhibiting the activity dependent transcription factor CREB in cervical neurons that are contacted by forelimb CST fibers in a mature circuit. **(B)** Left: 3D reconstruction of an example confocal image showing the analysis of contacted GFP+ neurons. A contact is indicated with an arrow, which identifies the GFP+ neuron as contacted. Right: quantification of the number of contacted GFP+ neurons in mice with CREB operational (-aCREB) versus inhibited (+aCREB) cervical neurons (p = 0.7186). Values are normalized to the number of GFP+ neurons and CST labeling. **(C)** Left: confocal maximum projection of exemplary forelimb CST collaterals in the cervical gray matter with bouton quantification indicated with arrows. Right: quantification of bouton density along cervical forelimb CST collaterals (p = 0.7830). **(D)** Quantification of the number of cervical forelimb CST collaterals exiting the white matter to enter the gray matter (p = 0.2764). Values are normalized to CST labeling. **(E)** Left: confocal maximum projection of exemplary cervical gray matter area where forelimb CST collaterals project to. Arrows indicate collaterals. Dotted line indicates white matter border. Right: quantification of the total length of all forelimb CST collaterals in the cervical gray matter (p = 0.7713). Values are normalized to forelimb CST labeling. Data analyzed using student's t test (two-tailed, unpaired). Bar lengths represent means, and error bars represent SEMs. Scale bars, 10µm in (B) and (C); 50µm in (E). Ctrl: control. ns: not significant. Two grouped independent experiments (n = 7-8 mice per experimental condition) with experimental setup shown in (A). Figure adapted, with permission from ref. [130].

GLOBALLY SILENCING SPINAL NEURON ACTIVITY DOES NOT ALTER CST REMODELING

Next, we investigated whether suppressing neuronal activity in cervical spinal neurons directly affects CST remodeling. We chemogenetically silenced neurons via activating expressed hM4Di receptors, inhibitory DREADDs, in the cervical spinal cord. Like in all DREADDs, hM4Di expression itself does not suppress neuronal activity. Only when a synthetic ligand, in this case CNO, is administered to the mouse and binds to the receptor, will the neuron be silenced. Thus, the same AAVs can be used for control and experimental conditions. This chemogenetic tool allows for temporal, when CNO is administered, and reversible, when CNO is metabolized, neuronal silencing.

hM4Di expression was induced by the injection of a mix of an anterograde AAV-DIO-hM4Di-mCherry and anterograde AAV-GFP-cre into the cervical spinal cord of C57Bl6 wildtype mice (Figure 17A). When neurons are infected with both AAVs, cre recombinase induced by AAV-GFP-cre will bind to the lox sites sequences of the other virus and result in the inversion of the flipped hM4Di-mCherry sequence. This intersectional targeting will lead to a successful expression of hM4Di, GFP, and mCherry. Since the same viruses were used for experimental and control animals they exhibited similar amounts of AAV infected neurons (-CNO: 119 ± 8 GFP positive neurons/section, +CNO: 119 ± 12 GFP positive neurons/section; n = 9 mice per group) and AAV expression patterns in the cervical cord (Figure 19F). Mice of different groups did, however, differ in drug administration; experimental mice received chronic, twice daily, CNO injections during the detour circuit formation phase (14dpi to 21dpi), whilst control animals received saline injections.

Surprisingly, global silencing of spinal neurons did not affect CST remodeling in all features analyzed. Mice that received chronic CNO injections exhibited similar amounts of contacted cervical spinal neurons as mice with mere saline injections (Figure 17B). Further, CST collateral morphology in the cervical spinal cord was also unaffected, in terms of bouton density (Figure 17C), total collateral length (Figure 17D), and number of exiting collaterals (Figure 17D and 19E).

SELECTIVELY SILENCING GLUTAMATERGIC SPINAL NEURON ACTIVITY ALTERS CST REMODELING

When globally silencing spinal neurons, we manipulated neurons irrespective of their involvement in CST detour circuit formation after SCI. To exclude neurons, not contained in the detour circuit, from the manipulation, we first investigated the population of neurons initially contacted by remodeling CST collaterals after a thoracic dorsal hemisection. For this purpose, we focused on two major neuronal populations of the cervical spinal cord, based on their neurotransmitter profile: excitatory, glutamatergic neurons and inhibitory, glycinergic neurons. To analyze CST contacts onto inhibitory spinal neurons we used a mouse line in which glycinergic neurons are labelled (GlyT2-GFP mice). Contacts onto glutamatergic spinal neurons were analyzed by cervically injecting an anterograde AAV, inducing cre dependent fluorescence, into a VGlut-cre mouse line, expressing cre in all glutamatergic cells. Our results show that three weeks after a thoracic dorsal hemisection, remodeling CST collaterals

preferentially contact excitatory, glutamatergic neurons in the cervical spinal cord. However, inhibitory, glycinergic neurons are barely contacted. (VGlut: 5.8 ± 1.47% of all cervical glutamatergic neurons contacted, GlyT2: 0.4 ± 0.06% of all cervical glycinergic neurons contacted; p = 0.0003, n = 12-15 mice per group).

Incorporating these results, we next specifically targeted glutamatergic neurons spontaneously contacted by remodeling CST collaterals. Therefore, we injected the anterograde AAV-DIO-hM4Di-mCherry into C4 of the VGlut-cre mouse line (Figure 17E). By using the same CNO administration scheme as described above, we, thus, silenced glutamatergic cervical spinal neurons chronically during the phase of detour circuit formation, after a thoracic dorsal hemisection. CNO administration did not affect AAV transduction, which was similar across control and experimental group (-CNO: 172 ± 9 mCherry positive neurons/section; +CNO: 174 ± 8 mCherry positive neurons/section; n =10-12 mice per group; Figure 19F). Due to the heterogeneous somatic labeling of neurons with DREADD-mCherry we stained the cervical spinal cord sections for NeuN. We, then, performed contact analyses on all neurons, as stained by NeuN, and later checked for their DREADD-mCherry positivity.

Specifically silencing cervical glutamatergic neurons during detour circuit formation resulted in a reduction in the number of manipulated neurons contacted by CST collaterals (Figure 17F). In addition, CST collaterals exhibited lower bouton density (Figure 17G), they were less numerous (Figure 17H and Figure 19E) and shorter in total (Figure 17I) when compared to controls with non-silenced cervical glutamatergic neurons. Thus, whilst globally silencing cervical neurons irrespective of their neurotransmitter identity during detour circuit formation does not affect CST remodeling after SCI, specifically silencing cervical glutamatergic neurons impaired CST remodeling in all aspects analyzed. These two sets of data highlight the differences between the effects of global and selective neuronal silencing on remodeling following SCI.

To extend our analysis on the effects of glutamatergic neuron silencing, we examined the number of contacts along CST collateral stretches that are in immediate vicinity of a cervical neuron (Figure 17J). Not only did the number of contacts per contacted neuron decrease by glutamatergic neuron silencing in the cervical cord (Figure 17J), but the contact density of a contacting collateral stretch was also reduced (Figure 17K). These data indicate that the already few silenced neurons that have CST collaterals in immediate vicinity, receive decreased synaptic input from the CST when compared to non-silenced neurons.

Next, we investigated if the degree of neuronal silencing of cervical glutamatergic neurons would gradually affect their likelihood of being contacted by remodeling CST collaterals. Alternatively, there could be a clear cutoff value in neuronal activity determining if a neuron would be contacted or not. After identifying all cervical neurons (NeuN positive) contacted by CST collaterals, we rendered their NeuN positive surfaces and measured their mCherry-hM4Di intensity inside the neuron, as an indicator for the degree of neuronal silencing (Figure 17L). The resulting quantification, in fact, shows that in mice treated with CNO, where DREADDs actively silenced cervical neurons, mCherry intensity within a neuron negatively correlates with the likelihood of that neuron being contacted (Figure 17M left). Remodeling CST collaterals even seemed to have partially compensated for the decrease in contacted neurons in

CNO treated mice by contacting more neurons that were mCherry negative when compared to control mice. Thus, the median mCherry intensity of contacted cervical neurons is significantly decreased in mice treated with CNO (Figure 17M right). When given a choice, remodeling CST collaterals will preferentially contact active rather than silent neurons. These results reinforce the idea that glutamatergic cervical neurons compete for input from remodeling CST collaterals after SCI by varying degrees of neuronal activity.

To check if further subpopulations of cervical excitatory neurons respond differently to modulating neuronal activity, we labeled LPSN by injection of the retrograde tracer Fluorogold into the lumbar spinal cord. As described in the introduction, after a thoracic hemisection the CST sprouts spontaneously to contact LPSN in the cervical cord, which provide a detour to denervated lumbar motoneurons. Silencing glutamatergic cervical neurons irrespective of any further identity also decreased the number of contacted LPSN (54.8% of control; n = 5-7 mice per group), which compares to the level of contact reduction onto all glutamatergic neurons (34.3 ± 8.6% of control; Figure 17F). Further, we observed a comparable reduction of contacted cells when we separately analyzed excitatory neurons located in different laminae of the CST projection area (57.7% of control for neurons in laminae V, 43.2% of control for neurons in laminae VI and 45.4% of control for neurons in laminae VII-VIII; control; n = 10-12 mice per group). Hence, the rules of activity dependent competition for input from remodeling CST collaterals apply as a general rule to various subpopulations of cervical glutamatergic neurons.

SILENCING A SPECIFIC NEURONAL SUBPOPULATION ALTERS CST REMODELING

To target a specific detour circuit, we selectively silenced LPSN by simultaneously injecting a retrograde AAV-cre into their lumbar projection area and an anterograde AAV-DIO-hM4Di-mCherry into their cervical origin in wildtype C57Bl6 mice (Figure 17N). To maximize the proportion of LPSN silenced, we adjusted our experimental approach from the one applied for silencing glutamatergic neurons: AAV expression time was increased by injecting AAVs before injury and sacrificing more than five weeks after injury, we injected AAVs at four locations cervically (spanning C4 to C6), and mice received chronic CNO injections for more than three weeks.

The AAV-DIO transfected the cervical spinal cords of experimental and control animals similarly (-CNO: 11.8 ± 0.6 mCherry positive neurons/section, +CNO: 12.5 ± 0.6 mCherry positive neurons/section; n = 7-8 mice per group) where mCherry positive LPSN cell bodies localized in the intermediate laminae (Figure 17O). Silencing LPSN chronically with CNO during detour circuit formation resulted in a decrease in total contacts between CST collaterals and mCherry-DREADD positive LPSN when compared to control mice (Figure 17P). This decrease consists of a change in contacts onto cell bodies as well as dendrites, indicating a change in general contact number but not contact distribution. Thus, silencing LPSN specifically during detour circuit formation also decreases their likelihood of receiving input from the remodeling CST after SCI.

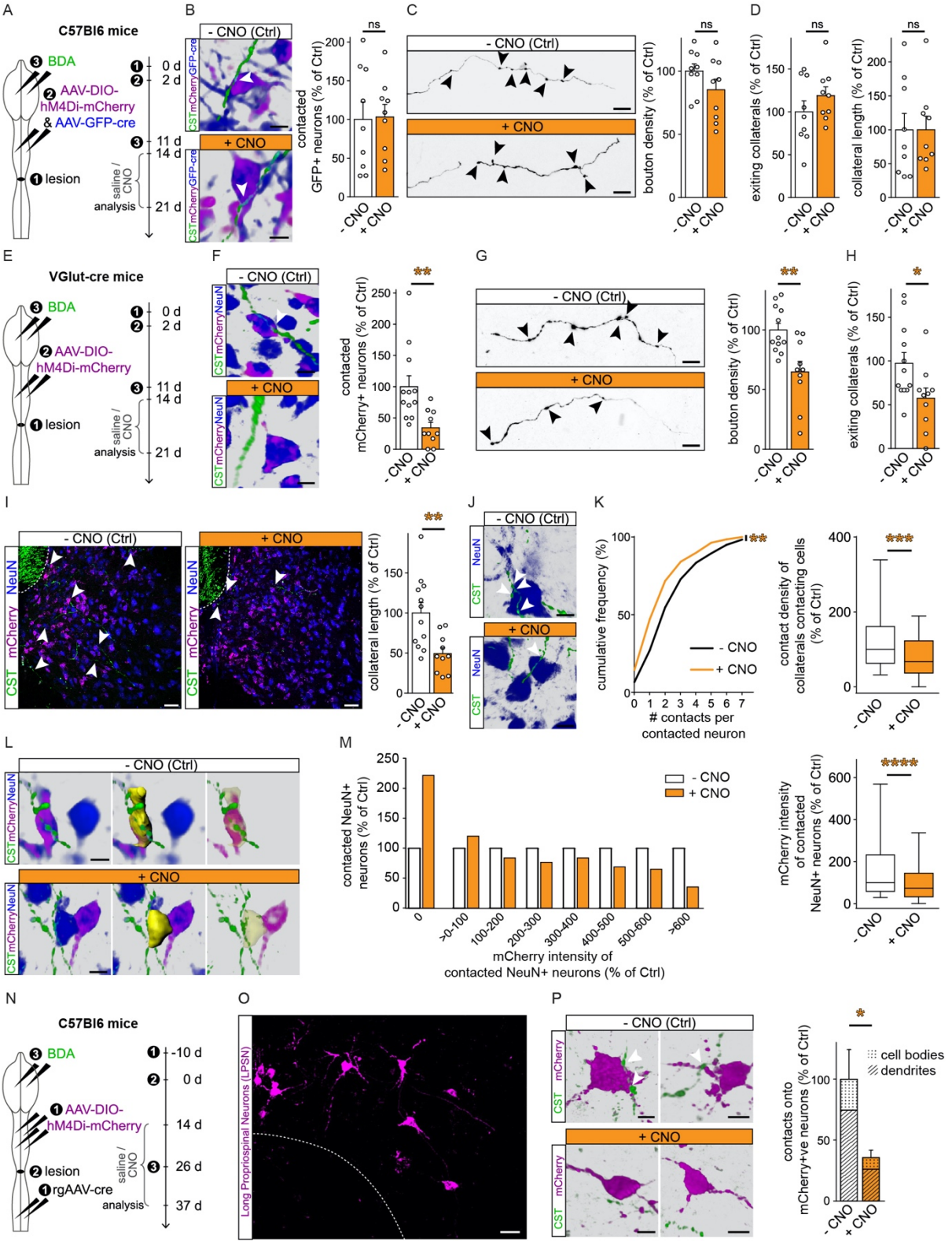

FIGURE 17 Activity dependent competition shapes detour circuit formation. **(A)** Experimental setup for chemogenetically silencing excitatory and inhibitory cervical neurons during detour circuit formation after a thoracic dorsal hemisection in C57Bl6 mice. **(B)** Left: 3D reconstruction of an example confocal image showing the analysis of contacted GFP+ neurons. A contact is indicated with an arrow, which identifies the GFP+ neuron as contacted. Right: quantification of the number of contacted GFP+ neurons in mice with non-silenced (-CNO) versus silenced (+CNO) cervical neurons ($p = 0.9079$). Values are normalized to the number of GFP+ neurons and CST labeling. **(C)** Left: confocal maximum projection of exemplary CST collaterals in the cervical gray matter with bouton quantification indicated with arrows. Right: quantification of bouton density along cervical CST collaterals ($p = 0.1651$). **(D)** Left: quantification of the number of cervical CST collaterals exiting the white matter to enter the gray matter ($p = 0.2682$). Right: quantification of the total length of all CST collaterals in the cervical gray matter ($p = 0.9980$). Values are normalized to CST labeling. **(E)** Experimental setup for chemogenetically silencing excitatory cervical neurons during detour circuit formation

after a thoracic dorsal hemisection in VGlut-cre mice. **(F)** Left: 3D reconstruction of an example confocal image showing the analysis of contacted mCherry+ neurons. Contacts were analyzed on NeuN stained neurons (arrow). Contacted NeuN+ neurons were then checked for mCherry positivity. Right: quantification of the number of contacted mCherry+ neurons in mice with non-silenced (-CNO) versus silenced (+CNO) excitatory cervical neurons ($p = 0.0049$). Values are normalized to the number of mCherry+ neurons and CST labeling. **(G)** Left: confocal maximum projection of exemplary CST collaterals in the cervical gray matter with bouton quantification indicated with arrows. Right: quantification of bouton density along cervical CST collaterals ($p = 0.0022$). **(H)** Quantification of the number of cervical CST collaterals exiting the white matter to enter the gray matter ($p = 0.0323$). Values are normalized to CST labeling. **(I)** Left: confocal maximum projection of exemplary cervical gray matter area where CST sprouting occurs. Arrows indicate collaterals. Dotted line indicates white matter border. Right: quantification of the total length of all CST collaterals in the cervical gray matter ($p = 0.0044$). Values are normalized to CST labeling. **(J)** 3D reconstruction of an example confocal image showing the analysis of contacts on CST collaterals in immediate vicinity of a contacted neuron. Arrows indicate boutons. **(K)** Left: quantification of the number of contacts per contacted neuron, presented as a cumulative frequency distribution ($p = 0.0037$, n = 138-181 contacted neurons). Right: quantification of bouton density along cervical CST collaterals in immediate vicinity of a contacted neuron ($p = 0.0001$, n = 138-181 contacted neurons). **(L)** 3D reconstruction of an example confocal image showing the analysis of mCherry-DREADD intensity within contacted neurons in Imaris. Surface rendering (in yellow) was performed on NeuN stained contacted neuron. **(M)** Left: histogram depicting the number of contacted neurons with a certain mCherry-DREADD intensity bin. Bin size is 100% of median intensity of all contacted neurons in control mice. 0% bin includes mCherry- neurons, which did not exhibit significantly higher intensities than the gray matter background (n = 368-1198 contacted neurons). Right: quantification of mCherry intensity per contacted neuron ($p < 0.0001$, n = 368-1198 contacted neurons). **(N)** Experimental setup for chemogenetically silencing LPSN during detour circuit formation after a thoracic dorsal hemisection. **(O)** Confocal maximum projection of exemplary cervical gray matter showing the distribution AAV infected LPSN. **(P)** Left: 3D reconstructions of example confocal images showing the analysis of contacts onto cell bodies (left image) and dendrites (right image) of mCherry+ neurons. Arrows indicate contacts. Right: quantification of the total number of contacts onto mCherry+ neurons in mice with non-silenced (-CNO) versus silenced (+CNO) LPSN ($p = 0.0312$). Values are normalized to the number of mCherry+ neurons and CST labeling. Contacts are further grouped into cell body (-CNO: 25.4%, +CNO, 26.8%) and dendritic (-CNO: 74.6%, +CNO, 73.2%) contacts (n = 41–134 contacts). Data in (B), (C), (D), (F), (G), (H), (I) and (P) analyzed using student's t test (two-tailed, unpaired). Bar lengths represent means, and error bars represent SEMs. Data in (K), right and (M), right analyzed using Mann-Whitney test. Median indicated by line. Whiskers represent the 10^{th} and 90^{th} percentile of mCherry intensity, and box borders represent the 25^{th} and 75^{th} percentile. Data in (K), left analyzed using Kolmogorov-Smirnov test. *$p < 0.05$, **$p < 0.01$, ***$p < 0.001$ and ****$p < 0.0001$. Scale bars, 10µm in (B), (C), (F), (G), (J), (L) and (P); 50µm in (I); 100µm in (O). Ctrl: control. ns: not significant. (B)–(D) two grouped independent experiments (n = 9 mice per experimental condition) with experimental setup shown in (A); (F)–(J) and (L)–(M) two grouped independent experiments (n = 10-12 mice per experimental condition), (K) one experiment (n = 5-7 mice per experimental condition) with experimental setup shown in (E); (O)–(P) one experiment (n = 7-8 mice per experimental condition) with experimental setup shown in (N). Figure adapted, with permission from ref. [130].

SELECTIVELY SILENCING GLUTAMATERGIC SPINAL NEURON ACTIVITY PREVENTS LOCOMOTOR RECOVERY

Lastly, we investigated whether manipulating neuronal activity and, thus, altering detour circuits would also affect locomotion as assessed by CatWalk experiments. We performed CatWalk experiments on mice with silenced cervical glutamatergic neuronal activity as we quantified furthest reaching anatomic changes after this manipulation. To maximize the number of glutamatergic neurons silenced, we injected an anterograde AAV-DIO-hM4Di-mCherry at four locations of the cervical spinal cord as performed in the LPSN silencing experiment (Figure 18A). To evaluate all crucial locomotor changes we assessed locomotor abilities with CatWalk at three time points: four days before injury, immediately after injury (3dpi), and chronically after injury and CNO or saline treatment (21dpi). To ensure that locomotion at 21dpi was explained by long-term alterations to the detour circuit, we stopped drug administration 24h before the behavioral testing at 20dpi. This experimental setup allowed us to eliminate potential short-term effects of CNO induced silencing of cervical glutamatergic neurons or off target effects of the drug.

To illustrate the CatWalk data and its calculated 177 parameters, we performed a PCA on experimental and control mice at our time point of interest, after chronic manipulation (21dpi). A two-dimensional representation of the data with PC1 and PC2 is shown in Figure 18B. Clearly, the PCA separated the control mouse group from the experimental one, illustrating that chronic neuronal silencing during detour circuit establishment affects locomotion. More precisely, the two groups significantly differ in PC1 (Figure 18C), which explains the biggest variance in the entire data set (30.5%).

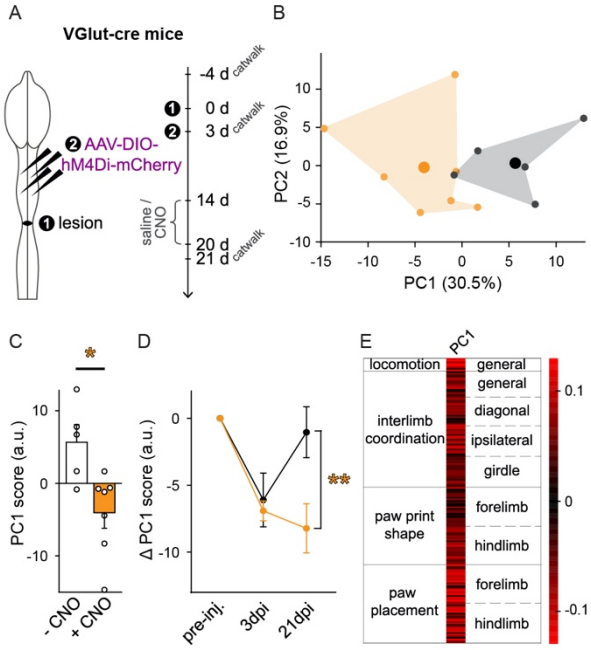

FIGURE 18 Selectively silencing excitatory spinal neuron activity prevents locomotor recovery. **(A)** Experimental setup for assessing motor skills after chemogenetically silencing excitatory cervical neurons during detour circuit formation after a thoracic dorsal hemisection. **(B)** PCA was applied on 177 parameters determined by the CatWalk at 21dpi. Each mouse with either non-silenced (-CNO, black) or silenced (+CNO, orange) excitatory cervical neurons is presented with a small dot in a new two-dimensional PC space. Big dots represent the mean of each group. **(C)** PC1 in one dimensional PC space ($p = 0.0140$). **(D)** Development of PC1 over time ($p = 0.0021$). PC1 was calculated for pre-injury and 3dpi time points using factor loadings from 21dpi. Values were normalized to pre-injury PC1. **(E)** Parameter clusters with color-coded factor loadings of PC1. Loadings close to 0, exhibiting low correlation with PC1 are coded in black, positive/negative loadings, exhibiting high correlation with PC1 are coded in red (scale on the right). Data in (C) analyzed using student's t test (two-tailed, unpaired). Bar lengths represent means, and error bars represent SEMs. Data in (D) analyzed using repeated two-way repeated-measures ANOVA and a Bonferroni post hoc test; dots represent means, and error bars represent SEMs. *$p < 0.05$, **$p < 0.01$. pre-inj.: pre-injury. a.u.: arbitrary units. One experiment (n = 5-7 mice per experimental condition) with experimental setup shown in (A). Figure adapted, with permission from ref. [130].

Having proven the difference, we next evaluated, whether chronic silencing during detour circuit formation improves or worsens locomotor behavior. We applied the PCA's calculated factor loadings of each parameter to each mouse' other time points to investigate how their locomotor abilities changed over time. To reduce intrasubject variability, we set pre-injury PC1 for each mouse as a baseline value and subtracted each time point from it. The resulting graph shows that both groups perform similarly right after the injury (Figure 18D). However, in the chronic time point saline treated mice recover motor skills to approximately pre-injury levels where CNO treated mice' motor skills remain impaired. Examining the factor loadings of PC1, or which parameters correlate with the PC, we identified several functional clusters. A broad range of parameters belonging to gross locomotion, ipsilateral interlimb coordination, hindlimb paw shape, and the timing of paw placement all explain the failure of SCI mice to recover after chronic CNO treatment. In summary, silencing cervical glutamatergic neurons chronically after SCI creates a defective detour circuit, preventing natural locomotor recovery in mice.

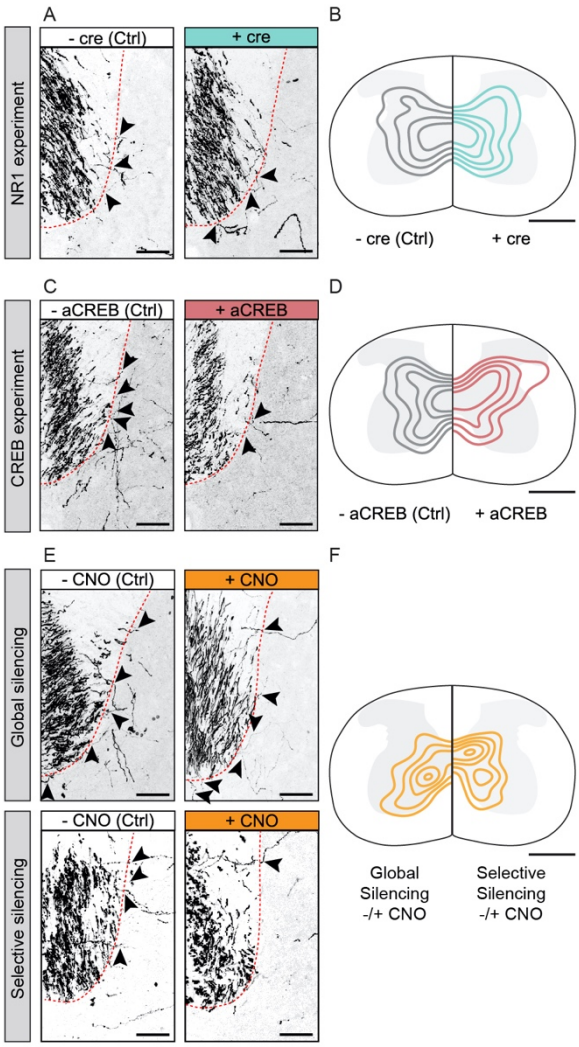

FIGURE 19 Exiting CST collaterals and similar distribution of AAV infected cells in control and experimental groups. **(A)** Confocal maximum projection of half of an exemplary cervical CST tract in mice with NMDAR functioning (-cre) versus nonfunctioning (+cre) cervical neurons during detour circuit formation. Arrows indicate exiting collaterals. Dotted line indicates white matter border. **(B)** Map showing distribution of GFP+ cervical neurons after AAV-GFP and AAV-GFP-cre injection. **(C)** Confocal maximum projection of half of an exemplary cervical CST tract in mice with CREB operational (-aCREB) versus inhibited (+aCREB) cervical neurons during detour circuit formation. Arrows indicate exiting collaterals. Dotted line indicates white matter border. **(D)** Map showing distribution of GFP+ cervical neurons after AAV-GFP and AAV-GFP-aCREB injection. **(E)** Confocal maximum projection of half of an exemplary cervical CST tract in mice with non-silenced (-CNO) versus silenced (+CNO) cervical neurons (top) or cervical excitatory neurons (bottom) during detour circuit formation. Arrows indicate exiting collaterals. Dotted line indicates white matter border. **(F)** Left side: Map showing distribution of mCherry+ cervical neurons after AAV-DIO-hM4Di-mCherry and AAV-GFP-cre injection into C57Bl6 mice. Right side: Map showing distribution of mCherry+ cervical neurons after AAV-DIO-hM4Di-mCherry injection into VGlut-cre mice. Scale bars, 50µm in (A), (C), and (E); 5mm in (B), (D), and (F). Ctrl: control. (B) one experiment (n = 4 per experimental condition) with experimental setup shown in Figure 13C and 15A. (D) two grouped independent experiments (n = 4 per experimental condition) with experimental setup shown in Figure 14A and 16A. (F), left one experiment (n = 4) with experimental setup shown in Figure 17A. (F), right one experiment (n = 4) with experimental setup shown in Figure 17E and 18A. Figure adapted, with permission from ref. [130].

DISCUSSION

For the first time, we provide evidence that activity dependent mechanisms guide remodeling after injury to the adult CNS. I formulated four thesis statements summarizing and interpreting our results to clarify the role of neuronal activity in CST remodeling after traumatic SCI. These statements will serve as a structure to the discussion of this thesis.

1. Neuronal activity dependent processes in the spinal cord are required for appropriate target selection during SCI induced remodeling.
2. There exists a critical window for activity dependent remodeling after SCI.
3. After SCI, the sprouting motor tract selects its target neurons based on their relative neuronal activity.
4. Neuronal activity in the spinal cord enables functional remodeling and allows for spontaneous motor recovery.

Circuit changes in the developing and uninjured adult CNS have also been shown to rely heavily on activity related processes. Each of my thesis statements is, thus, complemented by a comparison of detour with uninjured circuit formation, in the plastic adult and developing CNS. With this comparison, I will show how understanding a system's spontaneous attempt at recovery opens new possibilities for future research directions, novel disease intervention, and the improvement of current interventions. In closing, I explore the broader impact my dissertation might have on the research field of SCI, taking into account my chain of reasoning based on the literature analysis provided in the introduction and discussion, plus our research presented in the methodology and results section.

NEURONAL ACTIVITY DEPENDENT PROCESSES IN THE SPINAL CORD ARE REQUIRED FOR APPROPRIATE TARGET SELECTION DURING SCI INDUCED REMODELING

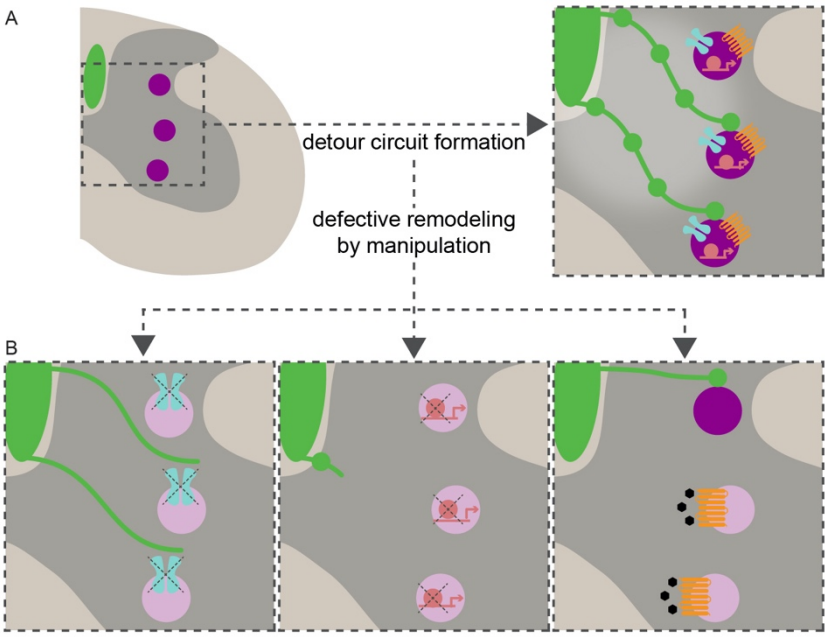

FIGURE 20 Interpretation of anatomic changes in the cervical spinal cord after manipulating activity dependent processes during detour circuit formation after SCI. **(A)** Without intervention the CST sprouts to contact unmanipulated target neurons in the cervical cord following a thoracic dorsal hemisection. **(B)** Left: when NMDAR in these target neurons are non-functional, CST collaterals do not form or even lose presynaptic bouton structures onto those cells. Middle: when CREB is inhibited, CST collaterals do not sprout or even retract, which results in a loss of contacts. Right: CST collaterals preferentially contact cells with high neuronal activity, i.e. low DREADD induced inhibition.

After SCI, we manipulated three neuronal activity dependent processes and identified their role in detour circuit formation. All genetically induced manipulations were performed in neurons of the cervical spinal cord at the location and time of hindlimb CST sprouting in response to a dorsal thoracic hemisection (Figure 7E, Figure 20A). [126] Manipulations during detour circuit formation all resulted in a reduction in contacts, which are usually formed spontaneously after SCI between sprouting hindlimb CST collaterals and cervical spinal neurons. For the first time, we show that inhibiting the function of activity dependent processes produces an anatomically defective detour circuit after CNS injury.

SYNAPTIC PLASTICITY IN THE (UN)INJURED ADULT CNS

Synaptic changes in the adult CNS also occur spontaneously without injury. Certain synapses are plastic, undergoing constant changes and redefining neural circuits, which forms the basis of learning and memory. Similar to remodeling processes after CNS injury, adult synaptic plasticity can be of functional or structural origin. [138] Functional changes strengthen or weaken synapses, and during structural changes synapses are either formed or removed. This synaptic plasticity is governed by different patterns of synaptic activity, defined by an interplay between pre- and postsynaptic activity. Rules of synaptic plasticity in the adult uninjured CNS exhibit noteworthy similarities to our observations concerning synaptic changes in the injured CNS.

Glutamate presents the main excitatory neurotransmitter in the spinal cord, [139] and it affects activity in the postsynaptic neuron by acting on various membrane receptors, such as NMDAR. The NMDAR's high permeability to calcium upon glutamate binding is pivotal in mediating synaptogenesis. Stimulating postsynaptic neurons of the adult hippocampus at low frequency [140] or antagonizing NMDARs [141], for example, leads to a reduction in hippocampal presynaptic bouton density. This structural synaptic plasticity is in line with the changes we observed after manipulating NMDARs in the injured CNS. After knocking out the NMDAR's crucial NR1 subunit in the cervical spinal cord during detour circuit formation, newly formed CST collaterals exhibited a reduction in contacts onto manipulated neurons (Figure 13). This effect extended to a reduction in presynaptic bouton structures on these CST collaterals (Figure 20B, left). NMDAR signaling is, therefore, critical for determining the number of boutons and the bouton's more downstream postsynaptic target selection during the formation of detour circuits in the injured CNS and during synaptic plasticity in the uninjured CNS.

Our *ex vivo* experimental setup does not give insight into bouton or contact dynamics. The observed reduction in contacts and boutons after suppressing NMDAR signaling could be explicable by a decreased formation or an increased elimination of synaptic structures. *In vivo* imaging in neuronal cell cultures has shown that NMDAR are recruited for synapse formation. [142] I, thus, hypothesize that during detour circuit formation, collaterals come into close apposition with NMDAR manipulated cervical neurons. The synapse, however, fails to recruit functional NMDARs to initiate the formation of a synaptic structure. An *in vivo* experiment could test this hypothesis and investigate whether adequate NMDAR signaling enables the formation of contacts or prevents their elimination.

The initiation of synaptic strengthening, i.e. functional rather than structural synaptic plasticity, in the adult CNS also depends on NMDAR signaling. [143–145] More specifically, NMDARs are essential for

long-term potentiation as well as long-term depression, which are considered key mechanisms of synaptic strengthening in learning and memory. [146] It is conceivable that NMDARs also play a role in processes of synaptic strengthening in detour circuits of the injured CNS. Knocking out the NR1 subunit during detour circuit formation might have affected the strength of the few synapses or boutons present. This analysis could be based on an extension of our bouton data by moving from a binary to a continuous scoring of boutons; apart from analyzing whether a bouton is present or absent, we could evaluate relative bouton changes in fluorescence intensity or size along a CST collateral. [147] In addition, synaptic strength could be assessed using an electrophysiological setup, electron microscopic images could be taken to identify the structure of synapses, or immunohistochemical staining for synaptic markers could be performed. This analysis would provide further insight into the effect NMDAR signaling exerts on the function of synaptic structures within SCI induced detour circuits.

After a new contact or synapse is formed it avoids being eliminated by consolidation for long-term integration into a circuit. Consolidating synaptic change demands new gene transcription and protein synthesis. [148,149] Previous studies have shown that some transcription factors are triggered by neuronal activity and thereby regulate complex gene expression profiles. [150] The activity dependent transcription factor CREB, for example, is considered to generally ensure maintenance of synaptic stability. [151,152] One study shows that relative CREB activity of a postsynaptic neuron determines its likelihood of being recruited into a memory trace. [151] Thus, where NMDAR signaling is involved in the initial stages of synaptic plasticity, i.e. synapse formation and initial strengthening, consolidation of synaptic change is determined by CREB activity.

CREB also plays a role in detour circuit formation following SCI (Figure 14). Inhibiting CREB resulted in a decrease in contacts between CST collaterals and manipulated cervical neurons, similar to the effects observed after NMDAR inhibition (Figure 20B, middle). Functional CREB mediated transcription and NMDAR signaling in the postsynaptic neuron are, thus, required for appropriate target finding of the remodeling CST after SCI. However, general CST collateral morphology, aside from contacts onto target neurons, is differentially shaped by these two activity dependent processes (Figure 20B, left and middle). In contrast to NMDAR inhibition, blocking CREB did not affect CST collateral bouton densities. In addition, we only observed a reduction in CST collateral branches innervating the cervical gray matter after blocking CREB. These differences in anatomic alterations illustrate that NMDAR and CREB do not function interchangeably but have slightly different roles in the activity dependent formation of detour circuits following SCI.

Taking together previous knowledge on synaptic plasticity in the uninjured CNS, I propose a model where a sequence of structural changes during detour circuit formation is determined by activity dependent processes. After a thoracic injury, CST collaterals sprout and form boutons close to neurons with functional NMDAR signaling. Afterwards, this bouton can mature into a synapse if a neuron with strong NMDAR signaling is contacted. The extent of CREB transcription, then, determines whether this contact together with its collateral branch is stabilized or not. Thus, when NMDAR signaling is inhibited, collaterals fail to initiate bouton formation and to find neurons to make contacts with. Remarkably, at our time of analysis, these CST collaterals remain in the cervical spinal cord, almost as if they were still searching for appropriate target neurons. It would be interesting to test, whether this anatomic state of

dense collaterals without boutons is permanent, or if, at some point, collaterals might be removed. When CREB is inhibited, I hypothesize that boutons and contacts form normally through functioning NMDAR signaling; only later, the CREB inhibited postsynaptic neuron fails to stabilize these contacts together with CST collaterals. These remodeled structures are consequently removed. I argue that in both, the uninjured and injured CNS, functional NMDAR signaling is necessary for the initiation of synaptic change and CREB for its consolidation.

PRUNING IN THE DEVELOPING AND INJURED CNS

Naturally, synaptic changes dominate not only adjustments within the adult CNS but also the CNS' entire development. During developmental circuit formation an excessive number of synapses is formed before synaptic elimination removes unnecessary synapses, whilst crucial ones are stabilized. This mechanism of establishing mature connectivity is called pruning and has been demonstrated in various locations of the CNS - at the neuromuscular junction, [153] in the visual [154,155] and olfactory system, [156] and in the cerebellum. [157] Pruning is a mechanism for synaptic target selection in the developing CNS.

Several studies in the developing CNS reveal the role of NMDAR signaling in pruning. Pharmacological intervention or genetic deletion of postsynaptic NMDAR [158–162] during development has been observed to impair synaptic pruning. All circuits exhibited aberrant synaptic patterning after inhibiting NMDARs. For example, deleting the NR1 subunit in the developing cortex, abolishes the somatotopic organization of the rodent barrel cortex. [158,161] Even in the developing peripheral nervous system, reducing NMDAR activation affects synaptic pruning on skeletal muscles. Usually, a muscle fiber is initially innervated by a large group of motor neurons, which reduces to innervation by one motor neuron later in development – a process significantly slowed down by decreasing NMDAR function. [162] These developmental studies show that NMDARs are crucial for adequate pruning by eliminating unnecessary connections and establishing mature synaptic patterning.

Pruning also occurs during detour circuit formation after SCI. In our investigated detour circuit, for example, previous data shows that after a thoracic hemisection CST collaterals sprout cervically and contact two populations of PSN, long and short ones. In contrast to LPSN, short PSN do not have connections to the lumbar target area of the lesioned CST and, thus, lack the potential to aid in motor recovery. At a later time point, during the pruning phase, unnecessary synapses onto short PSN get eliminated, whilst contacts onto LPSN are maintained. [126] The formation of excessive synaptic connections together with the later deletion of unnecessary ones determine the wiring of a mature detour circuit after CNS injury.

The mechanisms of pruning in detour circuits remain poorly understood. During detour circuit formation, our knockout of an NDMAR subunit led to a decrease in contacts between remodeling CST collaterals and the manipulated neurons. It would be interesting to investigate if our manipulation restricted to short PSN, during pruning of detour circuits, would affect contact numbers similarly. Due to the effects of NMDAR dysfunction on synapses during developmental pruning, it is conceivable that our manipulation would induce more contacts of sprouting CST collaterals onto spinal neurons because of

a failure to eliminate superfluous synapses onto the short PSN subpopulation. Experiments into the mechanisms of pruning could highlight how more contacts within a detour circuit does not necessarily lead to functional improvements, but that it is crucial for the system to differentiate between meaningful and meaningless connections to avoid maladaptive responses.

THERE EXISTS A CRITICAL WINDOW FOR ACTIVITY DEPENDENT REMODELING AFTER SCI

Next, we determined if the investigated circuitry was sensitive to the manipulation of activity dependent processes continuously, by varying the time of intervention. When manipulations occurred during the formation of detour circuits around two to three weeks post injury a defective detour circuit was created; manipulations in a mature detour circuit (Figure 15) or an intact one (Figure 16), however, did not impact circuitry. These results show that detour circuits only respond to changes in activity dependent processes with plasticity during a limited period of time after SCI.

Whilst plasticity in some areas of the CNS, like those associated with memory formation, reaches far into adulthood, the majority of areas lose their capacity to adapt after they have been fully established. In the cat visual system, for example, Hubel and Wiesel were the first to show that closing one eye and preventing it from exciting neurons during the first few months of life creates a visual cortex mainly representing the nondeprived eye. [163] This effect, however, is only exerted when the eye is closed in infant cats. Reopening the eye at a later time point does not reverse the anatomic effects. Thus, activity dependent plasticity in this area in cats is restricted to a certain period or critical window during development and infancy. Ocular dominance plasticity in the visual system is just one classical example of activity dependent circuit refinement that is temporally restricted to a developmental period; each CNS structure of each species has its own individual critical window. Only within this activity dependent critical window, can the different regions of the nervous system tailor their circuitry to the environment; after closing, circuitry in those regions remains unaffected by changes in activity.

Some researchers have linked the age dependent reduction in plasticity in certain regions of the CNS to a decline in CREB activity [164,165] and change in NMDAR function. [166,167] Further external suppression of these activity dependent processes in these mature areas would, thus, be in vain. Similarly, suppressing CREB in the cervical cord without injury did not affect forelimb CST collaterals and their contacts onto neurons in this region (Figure 16). Hence, adult CST circuitry is not *per se* plastic in the mature cervical cord or, at least, its plasticity does not depend on CREB function. In contrast, the suppression of CREB or NMDAR function around three weeks after SCI, severely affected hindlimb CST collaterals and their contacts onto neurons in this area. These experiments show that activity dependent remodeling and plasticity are reintroduced in specific areas through CNS injury. The cervical spinal cord, though, does not remain indefinitely plastic; later (twelve weeks post injury) manipulations of the NMDAR left the detour circuit unaltered. Together these data suggest that SCI reopens a critical window of plasticity and remodeling transiently, recapitulating developmental processes of activity, CREB and NMDAR dependence. However, this critical window will close after the detour circuit has been fully established.

It is important to note that these studies merely prove the existence of a critical window without defining its exact borders; it opens somewhere between directly after until two weeks after injury and closes between three and twelve weeks post injury. In order to narrow these periods down, more densely timed experiments would need to be conducted. For the design of SCI therapies that alter activity dependent processes in humans, it will also be important to determine the exact borders of the critical window. Remodeling will likely be most susceptible to interventions during this critical window.

Furthermore, it could be clinically relevant to explore whether established strategies that can reopen the critical window of developmental plasticity can be similarly employed to extend the phase of remodeling related plasticity after CNS injury. When a critical window can be reactivated, the application of interventions becomes less time sensitive. Interventions, then, do not need to be restricted to individuals with novel SCIs and immediate access to state-of-the-art medicine. Interestingly, the glial scar associated inhibitory factor, chondroitin sulphate proteoglycan, does not only impair axonal outgrowth in the injured CNS. Chondroitin sulphate proteoglycans have also been shown to inhibit the above described ocular dominance plasticity. Neutralizing these chondroitin sulphate proteoglycans in adult rodents with chondroitinase ABC reactivates the state of ocular dominance plasticity where the visual system is anatomically altered by monocular deprivation. [168] The success of chondroitinase ABC as a treatment for SCI might, hence, stem from a reopening of a critical window of remodeling related plasticity. Thus, extending or reactivating the critical period of plasticity during the formation of detour circuits after SCI, using remodeling supportive interventions such as chondroitinase ABC, and pairing these interventions with a manipulation of activity dependent processes might support remodeling beyond previous measurements.

AFTER SCI, THE SPROUTING MOTOR TRACT SELECTS ITS TARGET NEURONS BASED ON THEIR RELATIVE NEURONAL ACTIVITY

As a final anatomic assessment, we investigated the effect of direct silencing with DREADDs of different populations of cervical neurons during detour circuit formation (Figure 17). Global cervical silencing, irrespective of the neuronal population, did not alter the examined detour circuit. However, silencing neuronal activity similarly but specifically in glutamatergic cells or LPSN, which are normally contacted by remodeling CST collaterals, produced an anatomically defective detour circuit (Figure 20B, right). Further analyses after this manipulation revealed that DREADD levels determine each neuron's likelihood of being recruited for the emerging detour circuit. These results show that the effect of silencing neurons in the area of remodeling motor tracts after SCI depend on which neuronal population is targeted by the manipulation.

During synaptic refinement in development and synaptic plasticity in the adult uninjured CNS, global and selective manipulations of activity dependent processes have also been observed to affect circuitry differentially. For example, in hippocampal cultures, suppressing activity in a single neuron decreases its synaptic inputs, whereas broader populational suppression does not affect synapse formation. [169] In addition, nonuniform manipulations within a neuronal population provides further insight into plasticity determined by activity dependent processes. This experimental approach allows to relate

manipulation levels to the likelihood of a neuron to be integrated into a circuit. On a presynaptic level, for example, it was shown that axons compete to innervate a target by differences in relative neuronal activity. [170] Furthermore, as stated before, relative CREB function in potential target neurons determines which neurons will be integrated into an adult uninjured circuit. [151] This research suggests that is not total network activity that shapes circuitry. Rather, in the developing and adult, uninjured CNS, individual neurons within an eligible neuronal population compete for the integration into a circuit by relative strengths of activity dependent processes.

These experimental approaches and results from uninjured CNS compare to the ones from the injured CNS presented in this thesis. The contrast in anatomic effects by specific rather than global silencing indicates that spinal neurons are integrated into a detour circuit based on their relative activity. Silencing all neurons does not give one neuronal population a competitive advantage over another because total network activity rather than individual relative activity is reduced. However, specific silencing of cervical glutamatergic neurons or LPSN, which are usually contacted by remodeling collaterals, creates a defective detour circuit. These silenced populations exhibit less remodeled contacts because they have been set at a clear disadvantage to receive essential CST input. This interpretation is further supported by measuring the virally mediated mosaic expression of DREADDs within contacted neurons after glutamatergic silencing. We show that the higher the DREADD expression or the more silenced a neuron, the less likely it is to be contacted. We even observed a compensation effect, where after glutamatergic silencing CST collaterals increased their contacts onto unmanipulated neurons. In conclusion, after CNS injury, target selection during detour circuit formation is less determined by total network activity than by relative activity of an individual neuron and its competitors. Due to the comparable effect of silencing LPSN and glutamatergic neurons, I further postulate that this same rule of relative activity dependence similarly applies to the integration of all potential target cells. These interpretations suggest that measures to increase activity in a suitable neuronal population would be more promising in enhancing contact formation onto those neurons after SCI than bluntly increasing total network activity.

Our work demonstrates for the first time, that one can link relative DREADD expression levels to prominent anatomic alterations. How DREADD expression correlates with levels of neuronal silencing exactly is unclear. One hypothesis is simply that CNO can activate more DREADDs in high expressing cells and, therefore, induce stronger levels of hyperpolarization than in low expressing cells at a given moment. Another option is that highly expressing cells are silenced over a longer period of time, whilst neurons with lower DREADD expression levels are silenced more briefly due to a lack of receptor reserve. [171,172] Electrophysiological experiments or staining for markers of neuronal activity could shed light onto whether the degree of hyperpolarization or its duration is the driving force in our observed reduction in contacts after manipulation in detour circuits.

NEURONAL ACTIVITY IN THE SPINAL CORD ENABLES FUNCTIONAL REMODELING AND ALLOWS FOR SPONTANEOUS MOTOR RECOVERY

As stressed in the introduction of this thesis, functional assessment is indispensable when interpreting the effect of interventions. Using the CatWalk, we could show that the defect created by the manipulation of activity dependent processes during detour circuit formation was not limited to anatomy. More specifically, silencing glutamatergic neurons in the cervical spinal cord led to mice with chronically, up to three weeks post injury, impaired fine motor skills.

Firstly, this behavioral data identifies another circuit component crucial for spontaneous motor recovery after SCI. Anatomic remodeling alone does not imply functional improvements. In contrast, anatomic remodeling can even include miswiring, which causes further behavioral impairments like spasticity. Until now, relesioning the CST after a dorsal hemisection has only proven the motor tract's general ability to induce recovery, irrespective of the new connections it forms. [126] For the first time, we could show that the integration of cervical glutamatergic neurons into a detour circuit is key in functional remodeling after incomplete SCI.

It is possible that the CST is not the only remodeling motor tract that contacts cervical glutamatergic neurons. Thus, silencing those neurons might have a broader impact on other detour circuits, and the observed behavioral impairment results from a general decrease of contacts from several motor tracts. Unfortunately, there is no established technique, yet, to truly assign behavioral changes to the examined detour circuit; one would need to specifically silence or ablate a substantial number of synapses between hindlimb CST collaterals and cervical glutamatergic neurons.

The second insight gained from this experiment concerns the impact of neuronal activity dependent processes on functional remodeling after SCI. Anatomically, we observed the CST's attempt to compensate for the contact loss onto silenced cervical glutamatergic neurons by increasingly contacting unsilenced neurons. However, this anatomic effect does not result in a functional compensation, and mice with silenced glutamatergic neurons remain motorically impaired without exhibiting signs of spontaneous motor recovery. This seeming deviation could be explained in the anatomy, by the number of compensatory contacts being marginal or by the formation of superfluous contacts onto non-glutamatergic neurons that do not aid in functional recovery. By decreasing the viral infection rate in the cervical spinal cord, one could test if there is a percentage of silenced glutamatergic neurons, at which the detour circuit is able to compensate for a certain contact loss successfully, in terms of anatomy and function. Without these additional experiments, we can still conclude that glutamatergic neuronal activity at the location of motor tract sprouting after SCI is indispensable for spontaneous motor recovery.

Aberrant activity dependent processes have also been associated with functional deficits in the uninjured CNS; they have even been implicated in the etiology of several neurodevelopmental and neuropsychiatric disorders. [173,174] Increasing activity dependent processes like NMDAR [175–181] or CREB [182,183] function, on the contrary, has been applied to support synaptic plasticity and induce cognitive improvements. The enhanced performance of rodents was elicited in learning and memory tasks, such

as fear conditioning, fear memory, fear extinction, novel-object recognition, spatial memory, and working memory. Even in humans, upregulating NMDAR function has been observed to enhance performance in learning tasks. [184] Therefore, boosting activity dependent processes in the adult uninjured CNS is a promising approach to improve plastic processes and amplify functional abilities.

In my opinion, the most insightful follow-up study of our research investigates if increasing activity dependent processes in the injured CNS can also improve anatomic and functional remodeling. The first approach could be to increase downstream processes of neuronal activity, like NMDAR signaling and CREB transcription, in the cervical spinal cord after SCI. Secondly, our newly gained knowledge could aid in improving our methods of increasing neuronal activity directly as a potential treatment option for SCI. As described in the introduction of this thesis, a general increase of neuronal activity through rehabilitative training, electrostimulation, or pharmacological stimulation can improve locomotor recovery after CNS injury. In addition, a recent paper has shown that decreasing neuronal activity of spinal inhibitory neurons through DREADDs promotes functional recovery. [135] Combining these data with ours, their observed effect might have been induced by an increase in relative activity of glutamatergic neurons, placing them at a competitive advantage of receiving input from remodeling motor tracts. It remains to be revealed if targeting the increase of activity dependent processes to neurons, which are spontaneously contacted by remodeling collaterals of a detour circuit could further strengthen connectivity and improve functional recovery after SCI.

CLOSING REMARKS

In the introduction of my thesis, I have used previous studies to show that SCI is a devastating disease with far reaching implications and little prospect of relief for the individual affected and their community. The physiological and psychological impairments result from a damaging cascade induced at the injury site, leading to axon degeneration, demyelination, ischemia, cell death, inflammation and excitotoxicity. Unfortunately, the CNS fails to recover by regeneration during which axons attempt to regrow past the injury in vain. I have evaluated interventions that support axon regeneration as challenging because (1) the number of regenerating fibers and regeneration lengths achieved, so far, are limited, (2) regeneration itself without the formation of contacts cannot induce functional improvements, and (3) some of the observed functional improvements stem from off-target effects on remodeling, distal to the injury site.

Remodeling is the basis for the limited functional recovery we observe across species after incomplete SCI, and I have, thus, argued that it is a promising research field to design disease intervention. A detailed literature analysis on anatomic remodeling in rodents after SCI together with a presentation of the limitations of current interventions trying to boost remodeling, has underlined the importance to deepen our knowledge on processes involved in the spontaneous formation of detour circuits. Promising interventions, such as, pharmacological stimulation, epidural stimulation or neurorehabilitation converge in their effect of increasing neuronal activity in the spinal cord. We set out to investigate the exact impact neuronal activity dependent processes have on the formation of a well described detour circuit. This detour circuit is induced after a thoracic hemisection. Here, the CST

sprouts cervically to contact spinal neurons, such as LPSN. These neurons travel below the hemisection and contact initial target motoneurons of the injured CST, in the lumbar spinal cord.

By inhibiting NMDAR signaling, CREB function, and neuronal activity itself in the cervical spinal cord, we have shown that remodeling CST collaterals choose their target neurons based on the relative activity of these processes during a critical window of detour circuit formation. In addition to the anatomic regulation of remodeling, these activity dependent processes also enable functional remodeling and, thus, spontaneous locomotor recovery after SCI. Using these results, I have claimed that activity dependent neuronal competition guides functional and anatomic remodeling after CNS injury.

In the discussion, parallels between activity dependent neuroplasticity in the uninjured and injured CNS were drawn. A detailed literature analysis on plasticity in the developing and uninjured adult CNS has given rise to suggestions for future experiments that evaluate if certain observations extend to the spinal cord injured CNS. I have argued that the most urgent follow-up study would investigate if increasing activity dependent processes in a specific neuronal population during the critical window after SCI would boost remodeling and motor recovery.

In our study, we have unraveled some of the mechanisms by which the CNS partially and spontaneously compensates for SCI. Anatomic and functional remodeling after incomplete SCI is guided by activity dependent processes. Taken together, I have shown that deepening our understanding of a system’s spontaneous attempt at recovery, such as remodeling after CNS injury, identifies potential pitfalls that need to be considered when assessing treatment options and opens new possible entry points for the design of novel interventions.

REFERENCES

1. Hugenholtz H. Methylprednisolone for acute spinal cord injury: not a standard of care. *CMAJ*. 2003;168(9):1145-1146. http://www.ncbi.nlm.nih.gov/pubmed/12719318.

2. Bracken MB, Shepard MJ, Collins WF, et al. A Randomized Controlled Trial of Methylprenisolone Or Naloxone in the Treatment of Acute Spinal-Cord Injury. *N Engl J Med*. 1992;322(20):1405-1411. doi:10.1056/NEJM199312303292706

3. Bracken MB, Collins WF, Freeman DF, et al. Efficacy of methylprednisolone in acute spinal cord injury. *JAMA*. 1984;251(1):45-52. http://www.epistemonikos.org/documents/8ab883a6cf104f9308bd9fbb3384b07fdc3379af.

4. Hurlbert RJ. Methylprednisolone for acute spinal cord injury: an inappropriate standard of care. *J Neurosurg Spine*. 2000;93(1):1-7. doi:10.3171/spi.2000.93.1.0001

5. World Health Organization. *International Perspectives on Spinal Cord Injury*. Malta; 2013. https://apps.who.int/iris/bitstream/handle/10665/94190/9789241564663_eng.pdf;jsessionid=BE162937D1DC9820124E817B77A2883D?sequence=1.

6. Kraus JF, Franti CE, Riggins RS, Richards D, Borhani NO. Incidence of traumatic spinal cord lesions. *J Chronic Dis*. 1975;28(9):471-492. doi:10.1016/0021-9681(75)90057-0

7. DeVivo MJ, Kartus PL, Stover SL, Rutt RD, Fine PR. Cause of Death for Patients with Spinal Cord Injuries. *Arch Intern Med*. 1989;149:1761-1766. doi:10.1097/00132586-199006000-00043

8. Post MWM, Van Leeuwen CMC. Psychosocial issues in spinal cord injury: A review. *Spinal Cord*. 2012;50(5):382-389. doi:10.1038/sc.2011.182

9. Kennedy P, Rogers BA. Anxiety and depression after spinal cord injury: A longitudinal analysis. *Arch Phys Med Rehabil*. 2000;81(7):932-937. doi:10.1053/apmr.2000.5580

10. Noonan VK, Fingas M, Farry A, et al. Incidence and prevalence of spinal cord injury in Canada: A national perspective. *Neuroepidemiology*. 2012;38(4):219-226. doi:10.1159/000336014

11. Krueger H, Noonan VK, Trenaman LM, Joshi P, Rivers CS. The economic burden of traumatic spinal cord injury in Canada. *Chronic Dis Inj Can*. 2013;33(3):113-122. http://www.ncbi.nlm.nih.gov/pubmed/23735450.

12. Watson C, Paxinos G, Kayalioglu G. *The Spinal Cord: A Christopher and Dana Reeve Foundation Text and Atlas*. Academic press; 2009.

13. Sekhon LH, Fehlings MG. Epidemiology, demographics, and pathophysiology of acute spinal cord injury. *Spine (Phila Pa 1976)*. 2001;26:S2-12. doi:10.1097/00007632-200112151-00002

14. Tator CH, Duncan EG, Edmonds VE, Lapczak LI, Andrews DF. Changes in epidemiology of acute spinal cord injury from 1947 to 1981. *Surg Neurol*. 1993;40(3):207-215. doi:10.1016/0090-3019(93)90069-D

15. Kakulas B. A Review of the Neuropathology of Human Spinal Cord Injury with Emphasis on Special Features. *J Spinal Cord Med*. 1999;22(2):119-124. doi:10.1080/10790268.1999.11719557

16. Nathan PW. Effects on movement of surgical incisions into the human spinal cord. *Brain*. 1994;117:337-346. doi:10.1093/brain/117.2.337

17. Lemon RN. Descending Pathways in Motor Control. *Annu Rev Neurosci*. 2008;31:195-218. doi:10.1146/annurev.neuro.31.060407.125547

18. Schucht P, Raineteau O, Schwab ME, Fouad K. Anatomical Correlates of Locomotor Recovery Following Dorsal and Ventral Lesions of the Rat Spinal Cord. *Exp Neurol*. 2002;176(1):143-153. doi:10.1006/exnr.2002.7909

19. Williams PR, Marincu B-N, Sorbara CD, et al. A recoverable state of axon injury persists for hours after spinal cord contusion in vivo. *Nat Commun*. 2014;5:1-11. doi:10.1038/ncomms6683

20. Kerschensteiner M, Schwab ME, Lichtman JW, Misgeld T. In vivo imaging of axonal degeneration and regeneration in the injured spinal cord. *Nat Med*. 2005;11(5):572-577. doi:10.1038/nm1229

21. Lorenzana AO, Lee JK, Mui M, Chang A, Zheng B. A Surviving Intact Branch Stabilizes Remaining Axon Architecture after Injury as Revealed by InVivo Imaging in the Mouse Spinal Cord. *Neuron*. 2015;86(4):947-954. doi:10.1016/j.neuron.2015.03.061

22. Farrar MJ, Bernstein IM, Schlafer DH, Cleland TA, Fetcho JR, Schaffer CB. Chronic in vivo imaging in the mouse spinal cord using an implanted chamber. *Nat Methods*. 2012;9(3):297-302. doi:10.1038/nmeth.1856

23. Dray C, Rougon G, Debarbieux F. Quantitative analysis by in vivo imaging of the dynamics of vascular and axonal networks in injured mouse spinal cord. *Proc Natl Acad Sci U S A*. 2009;106(23):9459-9464. doi:10.1073/pnas.0900222106

24. Blight AR. Delayed demyelination and macrophage invasion: a candidate for secondary cell damage in spinal cord injury. *Cent Nerv Syst Trauma*. 1985;2(4):299-315. doi:10.1089/cns.1985.2.299

25. Gledhill RF, Harrison BM, McDonald WI. Demyelination and remyelination after acute spinal cord compression. *Exp Neurol*. 1973;38(3):472-487. doi:10.1016/0014-4886(73)90169-6

26. Irvine KA, Blakemore WF. Remyelination protects axons from demyelination-associated axon degeneration. *Brain*. 2008;131(6):1464-1477. doi:10.1093/brain/awn080

27. Noble LJ, Wrathall JR. Distribution and time course of protein extravasation in the rat spinal cord after contusive injury. *Brain Res*. 1989;482:57-66. doi:10.1016/0006-8993(89)90542-8

28. Popovich PG, Horner PJ, Mullin BB, Stokes BT. A quantitative spatial analysis of the blood-spinal cord barrier I. Permeability changes after experimental spinal contusion injury. *Exp Neurol*. 1996;142(2):258-275. doi:10.1006/exnr.1996.0196

29. Whetstone WD, Hsu JYC, Eisenberg M, Werb Z, Noble-Haeusslein LJ. Blood-spinal cord barrier after spinal cord injury: Relation to revascularization and wound healing. *J Neurosci Res*. 2003;74(2):227-239. doi:10.1002/jnr.10759

30. Franco R, Fernández-Suárez D. Alternatively activated microglia and macrophages in the central nervous system. *Prog Neurobiol*. 2015;131:65-86. doi:10.1016/j.pneurobio.2015.05.003

31. David S, Kroner A. Repertoire of microglial and macrophage responses after spinal cord injury. *Nat Rev Neurosci*. 2011;12(7):388-399. doi:10.1038/nrn3053

32. Nesic O, Perez-Polo R, Xu GY, et al. IL-1 receptor antagonist prevents apoptosis and caspase-3 activation after spinal cord injury. *J Neurotrauma*. 2001;18(9):947-956. doi:10.1089/089771501750451857

33. Ferguson AR, Christensen RN, Gensel JC, et al. Cell death after spinal cord injury is exacerbated by rapid TNF alpha-induced trafficking of GluR2-lacking AMPARs to the plasma membrane. *J Neurosci*. 2008;28(44):11391-11400. doi:10.1523/JNEUROSCI.3708-08.2008

34. Genovese T, Mazzon E, Crisafulli C, et al. TNF-α blockage in a mouse model of SCI: Evidence for improved outcome. *Shock*. 2008;29(1):32-41. doi:10.1097/shk.0b013e318059053a

35. Stirling DP, Cummins K, Mishra M, Teo W, Yong VW, Stys P. Toll-like receptor 2-mediated alternative activation of microglia is protective after spinal cord injury. *Brain*. 2014;137(3):707-723. doi:10.1093/brain/awt341

36. Jiang MH, Chung E, Chi GF, et al. Substance P induces M2-type macrophages after spinal cord injury. *Neuroreport*. 2012;23(13):786-792. doi:10.1097/WNR.0b013e3283572206

37. Kigerl KA, McGaughy VM, Popovich PG. Comparative analysis of lesion development and intraspinal inflammation in four strains of mice following spinal contusion injury. *J Comp Neurol*. 2006;494(4):578-594. doi:10.1002/cne.20827

38. Fenn AM, Hall JCE, Gensel JC, Popovich PG, Godbout JP. IL-4 signaling drives a unique arginase+/IL-1β+ microglia phenotype and recruits macrophages to the inflammatory CNS: consequences of age-related deficits in IL-4Rα after traumatic spinal cord injury. *J Neurosci*. 2014;34(26):8904-8917. doi:10.1523/JNEUROSCI.1146-14.2014

39. Zhang B, Bailey WM, Braun KJ, Gensel JC. Age decreases macrophage IL-10 expression: Implications for functional recovery and tissue repair in spinal cord injury. *Exp Neurol*. 2015;273:83-91. doi:10.1016/j.expneurol.2015.08.001

40. Li S, Stys PK. Mechanisms of ionotropic glutamate receptor-mediated excitotoxicity in isolated spinal cord white matter. *J Neurosci*. 2000;20(3):1190-1198. doi:10.1523/jneurosci.20-03-01190.2000

41. Liu D, Xu GY, Pan E, McAdoo DJ. Neurotoxicity of glutamate at the concentration released upon spinal cord injury. *Neuroscience*. 1999;93(4):1383-1389. doi:10.1016/S0306-4522(99)00278-X

42. Stirling DP, Stys PK. Mechanisms of axonal injury: internodal nanocomplexes and calcium deregulation. *Trends Mol Med*. 2010;16(4):160-170. doi:10.1016/j.molmed.2010.02.002

43. Alizadeh A, Dyck SM, Karimi-Abdolrezaee S. Traumatic Spinal Cord Injury: An Overview of Pathophysiology, Models and Acute Injury Mechanisms. *Front Neurol*. 2019;10(March):1-25. doi:10.3389/fneur.2019.00282

44. Wada S, Yone K, Ishidou Y, et al. Apoptosis following spinal cord injury in rats and preventative effect of N-methyl-D-aspartate receptor antagonist. *J Neurosurg*. 1999;91(1):98-104. doi:10.3171/spi.1999.91.1.0098

45. Fenrich KK, Weber P, Hocine M, Zalc M, Rougon G, Debarbieux F. Long-term in vivo imaging of normal and pathological mouse spinal cord with subcellular resolution using implanted glass windows. *J Physiol*. 2012;590(16):3665-3675. doi:10.1113/jphysiol.2012.230532

46. Bray GM, Villegas-Pérez MP, Vidal-Sanz M, Aguayo AJ. The use of peripheral nerve grafts to enhance neuronal survival, promote growth and permit terminal reconnections in the central nervous system of adult rats. *J Exp Biol*. 1987;132(1):5-19. http://www.ncbi.nlm.nih.gov/pubmed/3323406.

47. Neumann S, Woolf CJ. Regeneration of Dorsal Column Fibers into and beyond the Lesion Site following Adult Spinal Cord Injury. *Neuron*. 1999;23(1):83-91. doi:10.1016/S0896-6273(00)80755-2

48. Schwab ME, Thoenen H. Dissociated neurons regenerate into sciatic but not optic nerve explants in culture irrespective of neurotrophic factors. *J Neurosci*. 1985;5(9):2415-2423. doi:10.1523/JNEUROSCI.05-09-02415.1985.

49. Bregman BS, Kunkel-Bagden E, Schnell L, Dai HN, Gao D, Schwab ME. Recovery from spinal cord injury mediated by antibodies to neurite growth inhibitors. *Nature*. 1995;378(6556):498-501. doi:10.1038/378498a0

50. Simonen M, Pedersen V, Weinmann O, et al. Systemic deletion of the myelin-associated outgrowth inhibitor Nogo-A improves regenerative and plastic responses after spinal cord injury. *Neuron*. 2003;38(2):201-211. doi:10.1016/s0896-6273(03)00226-5

51. Cafferty WBJ, Duffy P, Huebner E, Strittmatter SM. MAG and OMgp synergize with Nogo-A to restrict axonal growth and neurological recovery after spinal cord trauma. *J Neurosci*. 2010;30(20):6825-6837. doi:10.1523/JNEUROSCI.6239-09.2010

52. Kim J-E, Li S, GrandPré T, Qiu D, Strittmatter SM. Axon Regeneration in Young Adult Mice Lacking Nogo-A/B. *Neuron*. 2003;38(2):187-199. doi:10.1016/S0896-6273(03)00147-8

53. Guest JD, Rao A, Olson L, Bunge MB, Bunge RP. The ability of human Schwann cell grafts to promote regeneration in the transected nude rat spinal cord. *Exp Neurol*. 1997;148(2):502-522. doi:10.1006/exnr.1997.6693

54. Sendtner M, Götz R, Holtmann B, Thoenen H. Endogenous ciliary neurotrophic factor is a lesion factor for axotomized motoneurons in adult mice. *J Neurosci*. 1997;17(18):6999-7006. doi:10.1523/JNEUROSCI.17-18-06999.1997

55. Acheson A, Barker PA, Alderson RF, Miller FD, Murphy RA. Detection of brain-derived neurotrophic factor-like activity in fibroblasts and Schwann cells: Inhibition by antibodies to NGF. *Neuron*. 1991;7(2):265-275. doi:10.1016/0896-6273(91)90265-2

56. Heumann R, Korsching S, Bandtlow C, Thoenen H. Changes of nerve growth factor synthesis in nonneuronal cells in response to sciatic nerve transection. *J Cell Biol*. 1987;104(6):1623-1631. doi:10.1083/jcb.104.6.1623

57. Bregman BS, McAtee M, Dai HN, Kuhn PL. Neurotrophic factors increase axonal growth after spinal cord injury and transplantation in the adult rat. *Exp Neurol*. 1997;148(2):475-494. doi:10.1006/exnr.1997.6705

58. Namiki J, Kojima A, Tator CH. Effect of Brain-Derived Neurotrophic Factor, Nerve Growth Factor, and Neurotrophin-3 on Functional Recovery and Regeneration After Spinal Cord Injury in Adult Rats. *J Neurotrauma*. 2000;17(12):1219-1231. doi:10.1089/neu.2000.17.1219

59. Schnell L, Schneider R, Kolbeck R, Barde Y-A, Schwab ME. Neurotrophin-3 enhances sprouting of corticospinal tract during development and after adult spinal cord lesion. *Nature*. 1994;367(6459):170-173. doi:10.1038/367170a0

60. Grill R, Murai K, Blesch A, Gage FH, Tuszynski MH. Cellular Delivery of Neurotrophin-3 Promotes Corticospinal Axonal Growth and Partial Functional Recovery after Spinal Cord Injury. *J Neurosci*. 1997;17(14):5560-5572. doi:10.1523/JNEUROSCI.17-14-05560.1997

61. Ye JH, Houle JD. Treatment of the chronically injured spinal cord with neurotrophic factors can promote axonal regeneration from supraspinal neurons. *Exp Neurol*. 1997;143(1):70-81. doi:10.1006/exnr.1996.6353

62. Kanno H, Pressman Y, Moody A, et al. Combination of Engineered Schwann Cell Grafts to Secrete Neurotrophin and Chondroitinase Promotes Axonal Regeneration and Locomotion after Spinal Cord Injury. *J Neurosci*. 2014;34(5):1838-1855. doi:10.1523/JNEUROSCI.2661-13.2014

63. Weidner N, Blesch A, Grill RJ, Tuszynski MH. Nerve growth factor-hypersecreting Schwann cell grafts augment and guide spinal cord axonal growth and remyelinate central nervous system axons in a phenotypically appropriate manner that correlates with expression of L1. *J Comp Neurol*. 1999;413(4):495-506. doi:10.1002/(SICI)1096-9861(19991101)413:4<495::AID-CNE1>3.0.CO;2-Z

64. Faulkner JR, Herrmann JE, Woo MJ, Tansey KE, Doan NB, Sofroniew M V. Reactive Astrocytes Protect Tissue and Preserve Function after Spinal Cord Injury. *J Neurosci*. 2004;24(9):2143-2155. doi:10.1523/JNEUROSCI.3547-03.2004

65. Herrmann JE, Imura T, Song B, et al. STAT3 is a Critical Regulator of Astrogliosis and Scar Formation after Spinal Cord Injury. *J Neurosci*. 2008;28(28):7231-7243. doi:10.1523/JNEUROSCI.1709-08.2008

66. Bundesen LQ, Scheel TA, Bregman BS, Kromer LF. Ephrin-B2 and EphB2 regulation of astrocyte-meningeal fibroblast interactions in response to spinal cord lesions in adult rats. *J Neurosci*. 2003;23(21):7789-7800. doi:10.1523/JNEUROSCI.23-21-07789.2003

67. Davies SJA, Fitch MT, Memberg SP, Hall AK, Raisman G, Silver J. Regeneration of adult axons in white matter tracts of the central nervous system. *Nature*. 1997;390(6661):680-683. doi:10.1038/37776

68. De Winter F, Oudega M, Lankhorst AJ, et al. Injury-induced class 3 semaphorin expression in

the rat spinal cord. *Exp Neurol*. 2002;175(1):61-75. doi:10.1006/exnr.2002.7884

69. Bradbury EJ, Moon LDF, Popat RJ, et al. Chondroitinase ABC promotes functional recovery after spinal cord injury. *Nature*. 2002;416(6881):636-640. doi:10.1038/416636a

70. Grimpe B, Silver J. A novel DNA enzyme reduces glycosaminoglycan chains in the glial scar and allows microtransplanted dorsal root ganglia axons to regenerate beyond lesions in the spinal cord. *J Neurosci*. 2004;24(6):1393-1397. doi:10.1523/JNEUROSCI.4986-03.2004

71. McKillop WM, Dragan M, Schedl A, Brown A. Conditional Sox9 ablation reduces chondroitin sulfate proteoglycan levels and improves motor function following spinal cord injury. *Glia*. 2013;61(2):164-177. doi:10.1002/glia.22424

72. Lu P, Wang Y, Graham L, et al. Long-distance growth and connectivity of neural stem cells after severe spinal cord injury. *Cell*. 2012;150(6):1264-1273. doi:10.1016/j.cell.2012.08.020

73. Bareyre FM, Garzorz N, Lang C, Misgeld T, Büning H, Kerschensteiner M. In vivo imaging reveals a phase-specific role of STAT3 during central and peripheral nervous system axon regeneration. *Proc Natl Acad Sci U S A*. 2011;108(15):6282-6287. doi:10.1073/pnas.1015239108

74. Blackmore MG, Wang Z, Lerch JK, et al. Krüppel-like Factor 7 engineered for transcriptional activation promotes axon regeneration in the adult corticospinal tract. *Proc Natl Acad Sci U S A*. 2012;109(19):7517-7522. doi:10.1073/pnas.1120684109

75. Park KK, Liu K, Hu Y, et al. Promoting Axon Regeneration in the Adult CNS by Modulation of the PTEN/mTOR Pathway. *Science*. 2008;322(5903):963-966. doi:10.1126/science.1161566

76. Liu K, Lu Y, Lee JK, et al. PTEN deletion enhances the regenerative ability of adult corticospinal neurons. *Nat Neurosci*. 2010;13(9):1075-1081. doi:10.1038/nn.2603

77. Parikh P, Hao Y, Hosseinkhani M, et al. Regeneration of axons in injured spinal cord by activation of bone morphogenetic protein/Smad1 signaling pathway in adult neurons. *Proc Natl Acad Sci U S A*. 2011;108(19):99-107. doi:10.1073/pnas.1100426108

78. Tang-Schomer MD, Patel AR, Baas PW, Smith DH. Mechanical breaking of microtubules in axons during dynamic stretch injury underlies delayed elasticity, microtubule disassembly, and axon degeneration. *FASEB J*. 2010;24(5):1401-1410. doi:10.1096/fj.09-142844

79. Erturk A, Hellal F, Enes J, Bradke F. Disorganized Microtubules Underlie the Formation of Retraction Bulbs and the Failure of Axonal Regeneration. *J Neurosci*. 2007;27(34):9169-9180. doi:10.1523/JNEUROSCI.0612-07.2007

80. Ruschel J, Hellal F, Flynn KC, et al. Systemic administration of epothilone B promotes axon regeneration after spinal cord injury. *Science*. 2015;348(6232):347-352. doi:10.1126/science.aaa2958

81. He M, Ding Y, Chu C, Tang J, Xiao Q, Luo Z-G. Autophagy induction stabilizes microtubules and promotes axon regeneration after spinal cord injury. *Proc Natl Acad Sci*. 2016;113(40):11324-11329. doi:10.1073/pnas.1611282113

82. Bradbury EJ, McMahon SB. Spinal cord repair strategies: why do they work? *Nat Rev Neurosci*. 2006;7(8):644-653. doi:10.1038/nrn1964

83. Anderson MA, O'Shea TM, Burda JE, et al. Required growth facilitators propel axon regeneration across complete spinal cord injury. *Nature*. 2018;561(7723):396-400. doi:10.1038/s41586-018-0467-6

84. Lang C, Bradley PM, Jacobi A, Kerschensteiner M, Bareyre FM. STAT3 promotes corticospinal remodelling and functional recovery after spinal cord injury. *EMBO Rep*. 2013;14(10):931-937. doi:10.1038/embor.2013.117

85. García-Alías G, Barkhuysen S, Buckle M, Fawcett JW. Chondroitinase ABC treatment opens a window of opportunity for task-specific rehabilitation. *Nat Neurosci*. 2009;12(9):1145-1151.

doi:10.1038/nn.2377

86. Steward O, Sharp K, Yee KM, Hofstadter M. A re-assessment of the effects of a Nogo-66 receptor antagonist on regenerative growth of axons and locomotor recovery after spinal cord injury in mice. *Exp Neurol*. 2008;209(2):446-468. doi:10.1016/j.expneurol.2007.12.010

87. Lee JK, Geoffroy CG, Chan AF, et al. Assessing Spinal Axon Regeneration and Sprouting in Nogo-, MAG-, and OMgp-Deficient Mice. *Neuron*. 2010;66(5):663-670. doi:10.1016/j.neuron.2010.05.002

88. Dietz V, Colombo G, Jensen L. Locomotor activity in spinal man. *Lancet*. 1994;344(8932):1260-1263. doi:10.1016/S0140-6736(94)90751-X

89. Wernig A, Müller S, Nanassy A, Cagol E. Laufband Therapy Based on'Rules of Spinal Locomotion'is Effective in Spinal Cord Injured Persons. *Eur J Neurosci*. 1995;7(4):823-829. doi:10.1111/j.1460-9568.1995.tb00686.x

90. Curt A, Bruehlmeier M, Leenders KL, Roelcke U, Dietz V. Differential effect of spinal cord injury and functional impairment on human brain activation. *J Neurotrauma*. 2002;19(1):43-51. doi:10.1089/089771502753460222

91. Wrigley PJ, Press SR, Gustin SM, et al. Neuropathic pain and primary somatosensory cortex reorganization following spinal cord injury. *Pain*. 2009;141(1-2):52-59. doi:10.1016/j.pain.2008.10.007

92. Henderson LA, Gustin SM, Macey PM, Wrigley PJ, Siddall PJ. Functional reorganization of the brain in humans following spinal cord injury: Evidence for underlying changes in cortical anatomy. *J Neurosci*. 2011;31(7):2630-2637. doi:10.1523/JNEUROSCI.2717-10.2011

93. Freund P, Weiskopf N, Ward NS, et al. Disability, atrophy and cortical reorganization following spinal cord injury. *Brain*. 2011;134(6):1610-1622. doi:10.1093/brain/awr093

94. Alkadhi H, Brugger P, Boendermaker SH, et al. What disconnection tells about motor imagery: Evidence from paraplegic patients. *Cereb Cortex*. 2005;15(2):131-140. doi:10.1093/cercor/bhh116

95. Hotz-Boendermaker S, Funk M, Summers P, et al. Preservation of motor programs in paraplegics as demonstrated by attempted and imagined foot movements. *Neuroimage*. 2008;39(1):383-394. doi:10.1016/j.neuroimage.2007.07.065

96. Curt A, Alkadhi H, Crelier GR, Hotz Boendermaker S, Hepp-Reymond MC, Kollias SS. Changes of non-affected upper limb cortical representation in paraplegic patients as assessed by fMRI. *Brain*. 2002;125(11):2567-2578. doi:10.1093/brain/awf250

97. Winchester P, McColl R, Querry R, et al. Changes in supraspinal activation patterns following robotic locomotor therapy in motor-incomplete spinal cord injury. *Neurorehabil Neural Repair*. 2005;19(4):313-324. doi:10.1177/1545968305281515

98. Cramer SC, Orr ELR, Cohen MJ, Lacourse MG. Effects of motor imagery training after chronic, complete spinal cord injury. *Exp Brain Res*. 2007;177(2):233-242. doi:10.1007/s00221-006-0662-9

99. Topka H, Cohen LG, Cole RA, Hallett M. Reorganization of corticospinal pathways following spinal cord injury. *Neurology*. 1991;41(8):1276-1283. doi:10.1212/wnl.41.8.1276

100. Streletz LJ, Belevich JKS, Jones SM, Bhushan A, Shah SH, Herbison GJ. Transcranial magnetic stimulation: Cortical motor maps in acute spinal cord injury. *Brain Topogr*. 1995;7(3):245-250. doi:10.1007/BF01202383

101. Freund P, Rothwell J, Craggs M, Thompson AJ, Bestmann S. Corticomotor representation to a human forearm muscle changes following cervical spinal cord injury. *Eur J Neurosci*. 2011;34(11):1839-1846. doi:10.1111/j.1460-9568.2011.07895.x

102. Thomas SL, Gorassini MA. Increases in corticospinal tract function by treadmill training after

incomplete spinal cord injury. *J Neurophysiol*. 2005;94(4):2844-2855. doi:10.1152/jn.00532.2005

103. Flor H, Denke C, Schaefer M, Grüsser S. Effect of sensory discrimination training on cortical reorganisation and phantom limb pain. *Lancet*. 2001;357(9270):1763-1764. doi:10.1016/S0140-6736(00)04890-X

104. Lotze M, Grodd W, Birbaumer N, Erb M, Huse E, Flor H. Does use of a myoelectric prosthesis prevent cortical reorganization and phantom limb pain? *Nat Neurosci*. 1999;2(6):501-502. doi:10.1038/9145

105. De Leon RD, Hodgson JA, Roy RR, Edgerton VR. Full Weight-Bearing Hindlimb Standing Following Stand Training in the Adult Spinal Cat. *J Neurophysiol*. 1998;80(1):83-91. doi:10.1152/jn.1998.80.1.83

106. Lovely RG, Gregor RJ, Roy RR, Edgerton VR. Effects of training on the recovery of full-weight-bearing stepping in the adult spinal cat. *Exp Neurol*. 1986;92(2):421-435. doi:10.1016/0014-4886(86)90094-4

107. Loy K, Schmalz A, Hoche T, et al. Enhanced voluntary exercise improves functional recovery following spinal cord injury by impacting the local neuroglial injury response and supporting the rewiring of supraspinal circuits. *J Neurotrauma*. 2018;35(24):2904-2915. doi:10.1089/neu.2017.5544

108. Engesser-Cesar C, Anderson AJ, Basso DM, Edgerton VR, Cotman CW. Voluntary wheel running improves recovery from a moderate spinal cord injury. *J Neurotrauma*. 2005;22(1):157-171. doi:10.1089/neu.2005.22.157

109. Engesser-Cesar C, Ichiyama RM, Nefas AL, et al. Wheel running following spinal cord injury improves locomotor recovery and stimulates serotonergic fiber growth. *Eur J Neurosci*. 2007;25(7):1931-1939. doi:10.1111/j.1460-9568.2007.05469.x

110. Bareyre FM, Kerschensteiner M, Misgeld T, Sanes JR. Transgenic labeling of the corticospinal tract for monitoring axonal responses to spinal cord injury. *Nat Med*. 2005;11(12):1355-1360. doi:10.1038/nm1331

111. Takeoka A, Vollenweider I, Courtine G, Arber S. Muscle Spindle Feedback Directs Locomotor Recovery and Circuit Reorganization after Spinal Cord Injury. *Cell*. 2014;159(7):1626-1639. doi:10.1016/j.cell.2014.11.019

112. Basso DM, Fisher LC, Anderson AJ, Jakeman LB, Mctigue DM, Popovich PG. Basso Mouse Scale for Locomotion Detects Differences in Recovery after Spinal Cord Injury in Five Common Mouse Strains. *J Neurotrauma*. 2006;23(5):635-659. doi:10.1089/neu.2006.23.635

113. Basso DM, Beattie MS, Bresnahan JC. A Sensitive and Reliable Locomotor Rating Scale for Open Field Testing in Rats. *J Neurotrauma*. 1995;12(1):1-21. doi:10.1089/neu.1995.12.1

114. Metz GA, Whishaw IQ. Cortical and subcortical lesions impair skilled walking in the ladder rung walking test: a new task to evaluate fore- and hindlimb stepping, placing, and co-ordination. *J Neurosci Methods*. 2002;115(2):169-179. doi:10.1016/s0165-0270(02)00012-2

115. Zörner B, Filli L, Starkey ML, et al. Profiling locomotor recovery: comprehensive quantification of impairments after CNS damage in rodents. *Nat Methods*. 2010;7(9):701-708. doi:10.1038/nmeth.1484

116. Hamers FPT, Koopmans GC, Joosten EAJ. CatWalk-assisted gait analysis in the assessment of spinal cord injury. *J Neurotrauma*. 2006;23(3-4):537-548. doi:10.1089/neu.2006.23.537

117. Takeoka A, Vollenweider I, Courtine G, Arber S. Muscle Spindle Feedback Directs Locomotor Recovery and Circuit Reorganization after Spinal Cord Injury. *Cell*. 2014;159(7):1626-1639. doi:10.1016/j.cell.2014.11.019

118. Ballermann M, Fouad K. Spontaneous locomotor recovery in spinal cord injured rats is accompanied by anatomical plasticity of reticulospinal fibers. *Eur J Neurosci*. 2006;23(8):1988-

1996. doi:10.1111/j.1460-9568.2006.04726.x

119. Zörner B, Bachmann LC, Filli L, et al. Chasing central nervous system plasticity: the brainstem's contribution to locomotor recovery in rats with spinal cord injury. *Brain*. 2014;137(6):1716-1732. doi:10.1093/brain/awu078

120. Asboth L, Friedli L, Beauparlant J, et al. Cortico–reticulo–spinal circuit reorganization enables functional recovery after severe spinal cord contusion. *Nat Neurosci*. 2018;21(4):576-588. doi:10.1038/s41593-018-0093-5

121. Courtine G, Song B, Roy RR, et al. Recovery of supraspinal control of stepping via indirect propriospinal relay connections after spinal cord injury. *Nat Med*. 2008;14(1):69-74. doi:10.1038/nm1682

122. Filli L, Engmann a. K, Zorner B, et al. Bridging the Gap: A Reticulo-Propriospinal Detour Bypassing an Incomplete Spinal Cord Injury. *J Neurosci*. 2014;34(40):13399-13410. doi:10.1523/JNEUROSCI.0701-14.2014

123. Weidner N, Ner A, Salimi N, Tuszynski MH. Spontaneous corticospinal axonal plasticity and functional recovery after adult central nervous system injury. *Proc Natl Acad Sci*. 2001;98(6):3513-3518. doi:10.1073/pnas.051626798

124. Ghosh A, Sydekum E, Haiss F, et al. Functional and anatomical reorganization of the sensory-motor cortex after incomplete spinal cord injury in adult rats. *J Neurosci*. 2009;29(39):12210-12219. doi:10.1523/JNEUROSCI.1828-09.2009

125. Fouad K, Pedersen V, Schwab ME, Brösamle C. Cervical sprouting of corticospinal fibers after thoracic spinal cord injury accompanies shifts in evoked motor responses. *Curr Biol*. 2001;11(22):1766-1770. doi:10.1016/S0960-9822(01)00535-8

126. Bareyre FM, Kerschensteiner M, Raineteau O, Mettenleiter TC, Weinmann O, Schwab ME. The injured spinal cord spontaneously forms a new intraspinal circuit in adult rats. *Nat Neurosci*. 2004;7(3):269-277. doi:10.1038/nn1195

127. Girgis J, Merrett D, Kirkland S, Metz GAS, Verge V, Fouad K. Reaching training in rats with spinal cord injury promotes plasticity and task specific recovery. *Brain*. 2007;130(11):2993-3003. doi:10.1093/brain/awm245

128. Maier IC, Baumann K, Thallmair M, Weinmann O, Scholl J, Schwab ME. Constraint-induced movement therapy in the adult rat after unilateral corticospinal tract injury. *J Neurosci*. 2008;28(38):9386-9403. doi:10.1523/JNEUROSCI.1697-08.2008

129. van den Brand R, Heutschi J, Barraud Q, et al. Restoring Voluntary Control of Locomotion after Paralyzing Spinal Cord Injury. *Science*. 2012;336(6085):1182-1185. doi:10.1126/science.1217416

130. Bradley PM, Denecke CK, Aljovic A, Schmalz A, Kerschensteiner M, Bareyre FM. Corticospinal circuit remodeling after central nervous system injury is dependent on neuronal activity. *J Exp Med*. 2019;216(11):2503-2514. doi:10.1084/jem.20181406

131. Vong L, Ye C, Yang Z, Choi B, Chua S, Lowell BB. Leptin Action on GABAergic Neurons Prevents Obesity and Reduces Inhibitory Tone to POMC Neurons. *Neuron*. 2011;71(1):142-154. doi:10.1016/j.neuron.2011.05.028

132. Zeilhofer HU, Studler B, Arabadzisz D, et al. Glycinergic neurons expressing enhanced green fluorescent protein in bacterial artificial chromosome transgenic mice. *J Comp Neurol*. 2005;482(2):123-141. doi:10.1002/cne.20349

133. Tsien JZ, Chen DF, Gerber D, et al. Subregion- and cell type-restricted gene knockout in mouse brain. *Cell*. 1996;87(7):1317-1326. doi:10.1016/s0092-8674(00)81826-7

134. Kakizawa S, Yamasaki M, Watanabe M, Kano M. Critical period for activity-dependent synapse elimination in developing cerebellum. *J Neurosci*. 2000;20(13):4954-4961. doi:10.1523/JNEUROSCI.20-13-04954.2000

135. Chen B, Li Y, Yu B, et al. Reactivation of Dormant Relay Pathways in Injured Spinal Cord by KCC2 Manipulations. *Cell*. 2018;174(3):521-535.e13. doi:10.1016/j.cell.2018.06.005

136. Metsalu T, Vilo J. ClustVis: a web tool for visualizing clustering of multivariate data using Principal Component Analysis and heatmap. *Nucleic Acids Res*. 2015;43(W1):W566-W570. doi:10.1093/nar/gkv468

137. Shepherd GMG, Harris KM. Three-dimensional structure and composition of CA3→CA1 axons in rat hippocampal slices: Implications for presynaptic connectivity and compartmentalization. *J Neurosci*. 1998;18(20):8300-8310. doi:10.1523/jneurosci.18-20-08300.1998

138. Holtmaat A, Svoboda K. Experience-dependent structural synaptic plasticity in the mammalian brain. *Nat Rev Neurosci*. 2009;10(9):647-658. doi:10.1038/nrn2699

139. Traynelis SF, Wollmuth LP, McBain CJ, et al. Glutamate receptor ion channels: structure, regulation, and function. *Pharmacol Rev*. 2010;62(3):405-496. doi:10.1124/pr.109.002451

140. Becker N, Wierenga CJ, Fonseca R, Bonhoeffer T, Nägerl UV. LTD Induction Causes Morphological Changes of Presynaptic Boutons and Reduces Their Contacts with Spines. *Neuron*. 2008;60(4):590-597. doi:10.1016/j.neuron.2008.09.018

141. Perez-Rando M, Castillo-Gómez E, Guirado R, et al. NMDA Receptors Regulate the Structural Plasticity of Spines and Axonal Boutons in Hippocampal Interneurons. *Front Cell Neurosci*. 2017;11(6):1-14. doi:10.3389/fncel.2017.00166

142. Washbourne P, Bennett JE, McAllister AK. Rapid recruitment of NMDA receptor transport packets to nascent synapses. *Nat Neurosci*. 2002;5(8):751-759. doi:10.1038/nn883

143. Malenka RC, Nicoll RA. Long-term potentiation - A decade of progress? *Science*. 1999;285(5435):1870-1874. doi:10.1126/science.285.5435.1870

144. Kerchner GA, Nicoll RA. Silent synapses and the emergence of a postsynaptic mechanism for LTP. *Nat Rev Neurosci*. 2008;9(11):813-825. doi:10.1038/nrn2501

145. Sawtell NB, Frenkel MY, Philpot BD, Nakazawa K, Tonegawa S, Bear MF. NMDA receptor-dependent ocular dominance plasticity in adult visual cortex. *Neuron*. 2003;38(6):977-985. doi:10.1016/s0896-6273(03)00323-4

146. Lau CG, Zukin RS. NMDA receptor trafficking in synaptic plasticity and neuropsychiatric disorders. *Nat Rev Neurosci*. 2007;8(6):413-426. doi:10.1038/nrn2153

147. Gala R, Lebrecht D, Sahlender DA, et al. Computer assisted detection of axonal bouton structural plasticity in in vivo time-lapse images. *Elife*. 2017;6:1-20. doi:10.7554/eLife.29315

148. Frey U, Krug M, Reymann KG, Matthies H. Anisomycin, an inhibitor of protein synthesis, blocks late phases of LTP phenomena in the hippocampal CA1 region in vitro. *Brain Res*. 1988;452(1-2):57-65. doi:10.1016/0006-8993(88)90008-x

149. Nguyen P, Abel T, Kandel E. Requirement of a critical period of transcription for induction of a late phase of LTP. *Science*. 1994;265(5175):1104-1107. doi:10.1126/science.8066450

150. Flavell SW, Greenberg ME. Signaling mechanisms linking neuronal activity to gene expression and plasticity of the nervous system. *Annu Rev Neurosci*. 2008;31:563-590. doi:10.1146/annurev.neuro.31.060407.125631

151. Han J-H, Kushner SA, Yiu AP, et al. Neuronal Competition and Selection During Memory Formation. *Science*. 2007;316(5823):457-460. doi:10.1126/science.1139438

152. Barco A, Alarcon JM, Kandel ER. Expression of constitutively active CREB protein facilitates the late phase of long-term potentiation by enhancing synaptic capture. *Cell*. 2002;108(5):689-703. doi:10.1016/s0092-8674(02)00657-8

153. Sanes JR, Lichtman JW. Development of the vertebrate neuromuscular junction. *Annu Rev Neurosci*. 1999;22(1):389-442. doi:10.1146/annurev.neuro.22.1.389

154. Katz LC, Shatz CJ. Synaptic activity and the construction of cortical circuits. *Science*. 1996;274(5290):1133-1138. doi:10.1126/science.274.5290.1133

155. Okawa H, Hoon M, Yoshimatsu T, Della Santina L, Wong ROL. Illuminating the Multifaceted Roles of Neurotransmission in Shaping Neuronal Circuitry. *Neuron*. 2014;83(6):1303-1318. doi:10.1016/j.neuron.2014.08.029

156. Yu CR, Power J, Barnea G, et al. Spontaneous Neural Activity Is Required for the Establishment and Maintenance of the Olfactory Sensory Map. *Neuron*. 2004;42(4):553-566. doi:10.1016/S0896-6273(04)00224-7

157. Hashimoto K, Ichikawa R, Kitamura K, Watanabe M, Kano M. Translocation of a “Winner” Climbing Fiber to the Purkinje Cell Dendrite and Subsequent Elimination of “Losers” from the Soma in Developing Cerebellum. *Neuron*. 2009;63(1):106-118. doi:10.1016/j.neuron.2009.06.008

158. Iwasato T, Datwani A, Wolf AM, et al. Cortex-restricted disruption of NMDAR1 impairs neuronal patterns in the barrel cortex. *Nature*. 2000;406(6797):726-731. doi:10.1038/35021059

159. Ultanir SK, Kim J-E, Hall BJ, Deerinck T, Ellisman M, Ghosh A. Regulation of spine morphology and spine density by NMDA receptor signaling in vivo. *Proc Natl Acad Sci U S A*. 2007;104(49):19553-19558. doi:10.1073/pnas.0704031104

160. Munz M, Gobert D, Schohl A, et al. Rapid Hebbian axonal remodeling mediated by visual stimulation. *Science*. 2014;344(6186):904-909. doi:10.1126/science.1251593

161. Arakawa H, Suzuki A, Zhao S, et al. Thalamic NMDA Receptor Function Is Necessary for Patterning of the Thalamocortical Somatosensory Map and for Sensorimotor Behaviors. *J Neurosci*. 2014;34(36):12001-12014. doi:10.1523/JNEUROSCI.1663-14.2014

162. Personius KE, Slusher BS, Udin SB. Neuromuscular NMDA Receptors Modulate Developmental Synapse Elimination. *J Neurosci*. 2016;36(34):8783-8789. doi:10.1523/JNEUROSCI.1181-16.2016

163. Hubel DH, Wiesel TN. The period of susceptibility to the physiological effects of unilateral eye closure in kittens. *J Physiol*. 1970;206(2):419-436. doi:10.1113/jphysiol.1970.sp009022

164. Pham TA, Rubenstein JLR, Silva AJ, Storm DR, Stryker MP. The CRE/CREB pathway is transiently expressed in thalamic circuit development and contributes to refinement of retinogeniculate axons. *Neuron*. 2001;31(3):409-420. doi:10.1016/S0896-6273(01)00381-6

165. Pham TA, Impey S, Storm DR, Stryker MP. Cre-mediated gene transcription in neocortical neuronal plasticity during the developmental critical period. *Neuron*. 1999;22(1):63-72. doi:10.1016/S0896-6273(00)80679-0

166. Fox K, Daw N, Sato H, Czepita D. Dark-rearing delays the loss of NMDA-receptor function in kitten visual cortex. *Nature*. 1991;350(6316):342-344. doi:10.1038/350342a0

167. Carmignoto G, Vicini S. Activity-dependent decrease in NMDA receptor responses during development of the visual cortex. *Science*. 1992;258(5084):1007-1011. doi:10.1126/science.1279803

168. Pizzorusso T, Medini P, Berardi N, Chierzi S, Fawcett JW, Maffei L. Reactivation of ocular dominance plasticity in the adult visual cortex. *Science*. 2002;298(5596):1248-1251. doi:10.1126/science.1072699

169. Burrone J, O’Byrne M, Murthy VN. Multiple forms of synaptic plasticity triggered by selective suppression of activity in individual neurons. *Nature*. 2002;420(6914):414-418. doi:10.1038/nature01242

170. Buffelli M, Burgess RW, Feng G, Lobe CG, Lichtman JW, Sanes JR. Genetic evidence that relative synaptic efficacy biases the outcome of synaptic competition. *Nature*. 2003;424(6947):430-434. doi:10.1038/nature01844

171. Ruffolo RR, Nichols AJ. The relationship of receptor reserve and agonist efficacy to the sensitivity of alpha-adrenoceptor-mediated vasopressor responses to inhibition by calcium channel antagonists. *Ann N Y Acad Sci*. 1988;522(1):361-376. doi:10.1111/j.1749-6632.1988.tb33377.x

172. Roth BL. DREADDs for Neuroscientists. *Neuron*. 2016;89(4):683-694. doi:10.1016/j.neuron.2016.01.040

173. Ebert DH, Greenberg ME. Activity-dependent neuronal signalling and autism spectrum disorder. *Nature*. 2013;493(7432):327-337. doi:10.1038/nature11860

174. Yap EL, Greenberg ME. Activity-Regulated Transcription: Bridging the Gap between Neural Activity and Behavior. *Neuron*. 2018;100(2):330-348. doi:10.1016/j.neuron.2018.10.013

175. Cao X, Cui Z, Feng R, et al. Maintenance of superior learning and memory function in NR2B transgenic mice during ageing. *Eur J Neurosci*. 2007;25(6):1815-1822. doi:10.1111/j.1460-9568.2007.05431.x

176. Tang YP, Shimizu E, Dube GR, et al. Genetic enhancement of learning and memory in mice. *Nature*. 1999;401(6748):63-69. doi:10.1038/43432

177. Wong RW-C, Setou M, Teng J, Takei Y, Hirokawa N. Overexpression of motor protein KIF17 enhances spatial and working memory in transgenic mice. *Proc Natl Acad Sci U S A*. 2002;99(22):14500-14505. doi:10.1073/pnas.222371099

178. Hawasli AH, Benavides DR, Nguyen C, et al. Cyclin-dependent kinase 5 governs learning and synaptic plasticity via control of NMDAR degradation. *Nat Neurosci*. 2007;10(7):880-886. doi:10.1038/nn1914

179. Manabe T, Noda Y, Mamiya T, et al. Facilitation of long-term potentiation and memory in mice lacking nociceptin receptors. *Nature*. 1998;394(6693):577-581. doi:10.1038/29073

180. Hawasli AH, Bibb JA. Alternative roles for Cdk5 in learning and synaptic plasticity. *Biotechnol J*. 2007;2(8):941-948. doi:10.1002/biot.200700093

181. Oomura Y, Hori N, Shiraishi T, et al. Leptin facilitates learning and memory performance and enhances hippocampal CA1 long-term potentiation and CaMK II phosphorylation in rats. *Peptides*. 2006;27(11):2738-2749. doi:10.1016/j.peptides.2006.07.001

182. Matynia A, Kushner SA, Silva AJ. Genetic approaches to molecular and cellular cognition: a focus on LTP and learning and memory. *Annu Rev Genet*. 2002;36:687-720. doi:10.1146/annurev.genet.36.062802.091007

183. Lee Y-S, Silva AJ. The molecular and cellular biology of enhanced cognition. *Nat Rev Neurosci*. 2009;10(2):126-140. doi:10.1038/nrn2572

184. Forsyth JK, Bachman P, Mathalon DH, Roach BJ, Asarnow RF. Augmenting NMDA receptor signaling boosts experience-dependent neuroplasticity in the adult human brain. *Proc Natl Acad Sci*. 2015;112(50):15331-15336.

185. Micheau A, Hoa D. vet-Anatomy. www.imaios.com. doi:10.37019/vet-anatomy

186. Martin JH. *Neuroanatomy: Text and Atlas*.; 1996.

ACKNOWLEDGEMENTS

First, I would like to thank the Spinal Cord Repair group of the Institute of Clinical Neuroimmunology. I was excellently supervised by Florence Bareyre, who guided me thoughtfully but also gave me the freedom to discover my own path and grow as a young scientist. I also thank Martin Kerschensteiner and Leda Dimou for their accurate and well-considered advice after presentations and during our TAC meetings.

Another crucial part of our research group is, of course, my colleagues who, after long days of seemingly endless analyses, became my friends, too. I especially thank Peter for sharing his project with me and for enduring/adding to our mostly weird lunch break-conversations. Laura, thank you for picking me up from the wrong address when I got lost on the day of my first interview with Florence. Who knows what would have happened without you? Maybe I would have done a 5-year PhD at the Döner place close by. Alex, thanks for the countless Monsters you provided me with, so I was too hyped on caffeine during most of my analyses. Mehrnoosh, thank you for being as loud and annoying as I am so that I didn't need to use the "I'm American, I'm allowed to be loud" - card as often. Almir, thank you for being one of my two anchors during the hardest part of my PhD and finding the right time to tell me that I was being a jerk.

This work was made possible by the Studienstiftung des deutschen Volkes and the Graduate School of Systemic Neuroscience who supported me ideologically and financially. I am grateful to have been given the opportunity to develop my skill set, to become an expert at a specialized research field and to just overall learn a lot.

Lastly, I would like to thank the people that will probably skip the whole first part of this thesis and only read the acknowledgements: my family. My parents' and brother's support were a prerequisite for all my achievements. I am lucky to have grown up with such inspiring and loving people. Naturally, I chose a partner that fits right in. Thomas, I hate not getting your input on these acknowledgements to include some of your kindness, wit and humor. Still, thank you for encouraging me in pursuing whatever I set out to do (even when I change my plans last minute). And above all, thank you for giving us our little bean who created the perfect ending to this journey and without whom this thesis would have been completed a year earlier.